Interim Progress Report on NASA Grant NAG5-2232

"Receiver Design, Performance Analysis, and Evaluation for Space-Borne Laser Altimeters and Space-to-Space Laser Ranging Systems"

for the period of April 15, 1996 to Oct. 14, 1996

Frederic M. Davidson
Xiaoli Sun
Christopher T. Field

Department of Electrical And Computer Engineering
The Johns Hopkins University
Baltimore, MD 21218

Abstract

This progress report consists of two separate reports. The first one describes our work on the use of variable gain amplifiers to increase the receiver dynamic range of space borne laser altimeters such as NASA's Geoscience Laser Altimeter Systems (GLAS). The requirement of the receiver dynamic range was first calculated. A breadboard variable gain amplifier circuit was made and the performance was fully characterized. The circuit will also be tested in flight on board the Shuttle Laser Altimeter (SLA-02) next year.

The second report describe our research on the master clock oscillator frequency calibration for space borne laser altimeter systems using GPS receivers.

October 1996

Design and Performance Measurement of the GLAS/SLA Variable Gain Amplifier Circuit

Xiaoli Sun

JHU and NASA/GSFC
June 27, 1996

1. Introduction

The received signals of a space borne laser altimeter varies over a broad range due to variation in the reflectivity and slope of the ground targets. The target reflectivity affects the received signal pulse energy, the slope affects the pulsewidth, and both affect the pulse amplitude. The photodetector and the subsequent amplifiers have to be able to accommodate the dynamic range of the received pulse amplitude, with sufficient gain to overcome the preamplifier noise but without saturation at anytime. Since the signal processing circuit such as an A/D converter usually has a limited input dynamic range, a variable gain amplifier (VGA) is necessary to achieve the optimal overall receiver performance.

We are currently developing a photodetector assembly for the Geoscience Laser Altimeter System (GLAS), which will include a wideband and wide control range VGA. The up coming Shuttle Laser Altimeter II (SLA-II) also requires a VGA in the photodetector assembly to improve the receiver dynamic range. We have built an engineering model VGA circuit card for SLA-II to substitute the first post amplifier card inside the detector assembly. Our test

results show that the circuit meets all the requirements for SLA-II. Its performance also exceeds the VGA requirement for GLAS.

The rest of this report describes the details of the VGA requirement for GLAS and SLA-II and a proposed GLAS detector assembly circuit design which includes a photodetector preamplifier module, a VGA, a low power amplifier, and a power amplifier. Lastly, the design and the test results of the SLA-II VGA circuit card will be presented.

2. Signal Dynamic Range Requirement for GLAS

The expected signal level at the GLAS altimeter receiver is 1.45 fJ (7760 photons) per pulse incident to the photodetector, assuming 80 cm diameter telescope, 25 cm diameter center obscuration, 100 mJ laser pulse energy, 20% target reflectivity, 705 km altitude orbit, 50% optics transmission, and 50% round trip atmosphere transmission[1]. The peak received signal power is given as the received pulse energy divided by the pulse width. The most likely received pulse width is 30 ns FWHM, which corresponds to a 3 degree slope ground target and 70 m laser footprint. The received peak power under this pulse width is, therefore, 1.45fJ/30ns = 48.3 nW.

The peak signal power can increase by 24 times (27.6dB) when GLAS is over flat ice sheet with 80% reflectivity and 5 ns received pulse width. Note it is the signal peak power that we have to accommodate without saturation and to give an output signal which is within the optimal range for the subsequent signal processing circuit.

---

[1] see the attached link margin analysis.

The lowest signal peak power to be considered should be the same as the minimum detectable signal, which is about 130 photons/pulse for 30 ns FWHM at nighttime. The minimum detectable signal level also increases with the received pulse width, but we consider only 30 ns here as the typical case. The overall input signal range to be considered is, therefore, 7760/130 times 24, or a factor of 1400 (63dB) for nighttime. As a comparison, the range for daytime is a factor of 470 (53dB).

To achieve the optimal receiver performance, the VGA gain adjustment range plus the optimal input signal range for the subsequent signal processing circuitry such as a waveform digitizer should be greater than or equal to the maximum input signal range at nighttime. For a 8 bit waveform digitizer, the optimal input signal lies between 1/16 to 1/2 the full scale (4-7 bits out of the full 8 bits) based on our analysis and the experimental results[2], which gives an optimal input range of 8, or 18 dB. One can further narrow the required VGA range by another factor of 2 (6 dB) because the signal level into the waveform digitizer can be lower than the optimal level for weak signal when other noise sources dominate that 3 bits A/D resolution is sufficient[3]. Therefore, the VGA range can be as low as 39 dB.

---

[2] X. Sun, "Design and Performance Measurement of the GLAS Breadboard Altimeter Receiver," Interim Progress Report on NASA Grant NAG5-2232, "Receiver Design, Performance Analysis, and Evaluation for Space-Borne Laser Altimeters and Space-to-Space Laser Ranging Systems," for the period of Oct. 16, 1995 to April 14, 1996, Dept. ECE, The Johns Hopkins University, Baltimore, MD 21218.

[3] Same as above.

Another 3 dB reduction in the VGA range could be obtained if one designed the photodetector preamplifier such that the impulse response matches the received optical signal pulse that the output pulse width is $\sqrt{2}$ that of the input. However, this is difficult to achieve in practice, because the primary goal of the preamplifier is low noise and wide band, preferably not to be complicated by the impulse response pulse shape.

The electrical bandwidth of the VGA and the subsequent amplifiers have to be wide enough to pass the shortest possible received laser pulses, 5 ns FWHM. The APD preamplifier module has a 3 dB bandwidth of about 150 MHz with a RC filter type roll-off. The subsequent amplifiers should all have similar or wider bandwidth.

The gain of the photodetector preamplifier hybrid module for GLAS is about 200 kV/W. The output dynamic range is greater than 60 dB according our previous test results. The output pulse amplitude in response to the 1.45fJ /30 ns pulse is roughly 10 mV. The optimal input signal range for a waveform digitizer is typically about 0.5 volt (mid scale). Usually the signal output from the detector assembly is split between the waveform digitizer and other branches of the receiver such as the time interval unit (TIU). The desired signal amplitude from the detector assembly should be about 1 volts. Consequently, the design goal for the detector post amplifiers including the VGA should be 40 dB nominal gain, variable by at least +12 to -28 dB (40dB range), with a roughly 10 mV nominal input and 1 volt output pulse amplitude (13dBm into 50Ω).

Usually a VGA and several linear amplifiers have to be used in cascade to achieve this goal.

3. VGA Requirement for SLA-II

SLA-II is similar to GLAS except for the lower orbit altitude, 310 km, smaller telescope diameter, 40 cm, lower transmitted laser pulse energy, 40 mJ/pulse, and wider transmitted laser pulse width, 10 ns. The expected received signal level for 0.20 reflectivity target is 0.52 times that of GLAS, or 0.75 fJ/pulse (4040 photons). The peak optical signal power for 30 ns FWHM pulses is 25 nW. The maximum input signal is 12 (21.6dB) times higher when it is over flat ice or snow ground target (0.8 reflectivity and 10 ns pulse width). The minimum detectable signal is roughly the same as SLA–II (130 photons/30ns pulse). The input signal dynamic range is, therefore, 370 or 51 dB. The optimal input signal range for the waveform digitizer and TIU should be the same as GLAS, 18+6=24 dB. Therefore, the VGA range required is about 27 dB.

The 3dB bandwidth required for the SLA detector is greater than 75 MHz to pass 10 ns FWHM pulses.

The control signal needs to be 0-5 volts since a D/A control signal from the on board computer is readily available in the current system. The DC power supplies are preferred to be ±12 V.

The APD preamplifier hybrid module has a gain of 775 kV/W. The output pulse amplitude at 30 ns FWHM is 19.4 mV. The optimal output signal amplitude from the second stage should be about

2 volts, which leads to a total of 40 dB gain of the entire detector assembly. At present, SLA detector assembly has two post amplifier stages, one has a voltage gain of 24.2 (27.7dB) and the other 10 (20dB). We can just replace the first amplifier stage with a VGA circuit card and leave the second stage unchanged. Consequently, we need a VGA circuit card of 20 dB nominal gain and variable by +5 to -22 dB with a nominal input signal of about 20 mV.

4. Proposed GLAS Detector Post Amplifier Circuit

One candidate VGA for both GLAS and SLA is the wideband AGC amplifier, Model SL6140 by GEC Plessey Semiconductors[4]. It has a gain from at least -32 to 15 dB, a 53 dB range with 50 Ω load (70 dB specified for 1KΩ load), 400 MHz bandwidth, and a maximum output amplitude of 600 mV into 50 Ω load (8.6dBm).

One candidate for the last stage is wideband low distortion power amplifier, CLC561 by Comlinear Corp. It has a 3 dB bandwidth of 150 MHz at +24dBm output level (10V peak to peak). The gain can be set to as high as 26 dB without significant reduction in the bandwidth.

To achieve the required gain and variation range, 40 dB plus 12 minus 28 dB, one can set the nominal VGA gain to 0 dB and use another 14 dB low power amplifier before or after the VGA. This type of linear amplifiers are relatively easy to find. One candidate is the GEC Plessey SL560 or its equivalence, which has a bandwidth of 300 MHz and a gain of 14 dB[5].

---

[4] see the attached data sheets.

[5] See the attached data sheets.

5. Engineering Model VGA Circuit Card for SLA-II and the Test Results

We have built an engineering model VGA circuit card for SLA-II, to replace the post amplifier #1 card inside the detector assembly. The circuit consists of a GEC Plessey SL6140 VGA amplifier followed by an SL560 linear amplifier. Figure 1 shows the circuit schematic. The circuit is actually part of the amplifier chain which we proposed for the GLAS detector assembly in the previous section. The circuit was fully tested and well met all of our design goals.

The entire circuit was operated from a single +12V power supply. The SL560 amplifier required a lower supply voltage and a 150 Ω resister was used to drop the 12 volt supply to the desired 6-9 volts range. The current drawn by this amplifier was 30 mA. The VGA stage drew 18 mA. The total power consumption of the card was 580 mW.

Figure 2 shows a block diagram of test setup. The input signal consists of 20 ns wide rectangular pulses. The oscilloscope monitored simultaneously both the output and the input (times 10 due to the 20 dB pad) and measured the pulse parameters. The VGA control voltage was generated by a programmable power supply.

Figure 3 gives a spreadsheet of the test conditions and the results. Figure 4 plots the voltage gain and the relative propagation delay vs. control voltage. We have achieved a gain control range from -23 to 30 dB, well exceeded the range required by SLA-II (-22 to 5 dB). The propagation delay varied by no more than 0.5 ns over the entire gain

range. The maximum output pulse amplitude was found to be about 600 mV.

Figure 5 shows the input and the output pulse at close to the maximum gain. It shows the circuit has a rise and fall times within 2.4 ns. There was little pulse overshoot and undershoot. Figures 6 through 9 show the measured input and output pulses at maximum, 10, 1, and 0.1 voltage gain settings. At very low gain, the output has some overshoot and undershoot, as shown in Figure 9.

Figure 10 shows the input and the output pulse shapes at individual amplifier stages. The VGA stage output looked noisy because of the oscilloscope probe. The gain of the linear amplifier (called "buffer") after the VGA is shown to be 14.5 dB. The gain of the VGA stage is, therefore, -37.5 to 15.5 dB.

Figure 11 shows the slight pulse undershoot due to AC coupling for relatively wide pulses, 1 μs in this case. The AC coupling capacitors were 0.47 μF. Since the input and output impedance were 50 Ω , the 3 dB lower cutoff frequency was about 6.8 kHz, which was the same as the rest of the detector assembly. The lower cutoff frequency can be reduced by increasing the capacitance or using two or three of those capacitors in parallel.

We also measured the VGA response time to the control signal by feeding it with a 2 MHz pulse train and applying a step signal to the control terminal. The bypass capacitor, C3, was temporally removed during this measurement. Figures 12 and 13 show the measurement results. The response time of the VGA was less than 0.5 μs without

any ringing. Therefore, we are capable of changing the detector assembly gain on a pulse to pulse base for both SLA-II and GLAS. Currently, the VGA response time was set to about 1 ms with the use of a 0.1 μF bypass capacitor.

Figures 14,15, and 16 show the S-parameter measured with our HP8753C/85047 network analyzer from 300 kHz to 500 MHz. The 3 dB bandwidth of the circuit is shown to be about 300 MHz and the phase response was very close to linear. The input voltage standing wave ratio (VSWR) was less than 1.25:1, mostly because of the 50 Ω resistor at the input. The output stage inside SL560 was an emitter follower, which had a very low source impedance and the measured S_{22} was not shown here.

Lastly, Figure 17 shows the measured quiescent output noise spectrum measured by the HP3585A and HP8561B spectrum analyzer. The average spectral density was -128 dBm/Hz, which corresponded to 1.54 mV rms on a 50 Ω load over the 300 MHz bandwidth, which was about what we saw on the oscilloscope during the test. The highest noise spikes within the 300 MHz bandwidth were -65 dBm at about 20 MHz, which corresponded to an insignificant 0.1.3 mV rms in time domain. Note the circuit card was not well shielded during this test and the spikes might have come from RF pick-up from the environment.

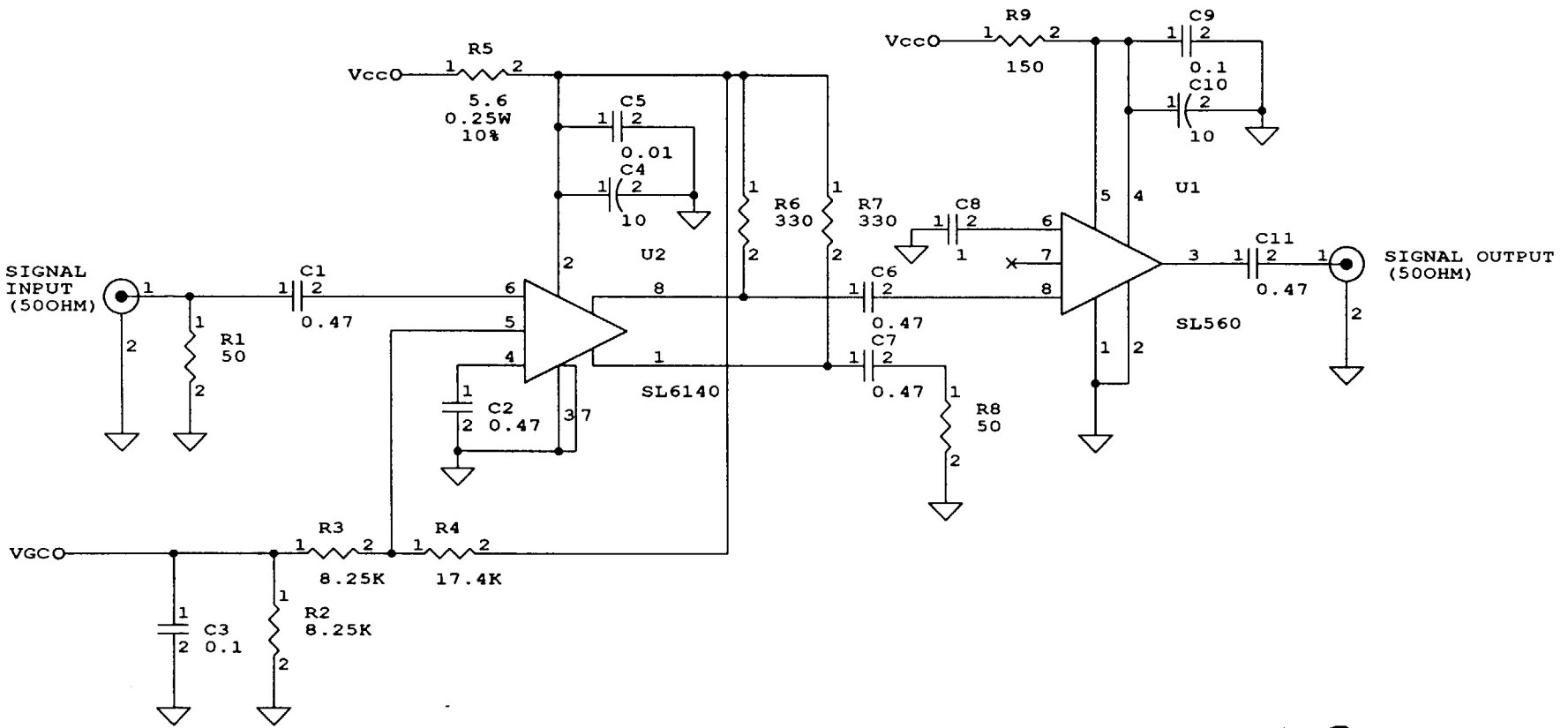

Fig. 1. Circuit Schematics of SLA-2 VGA card.

NOTES:
1) ALL CAPACITANCE VALUES IN uF
2) ALL RESISTANCE VALUES IN OHMS
3) ALL CAPACITORS 50V, 10% TOL.
4) ALL RESISTORS 0.125W, 2% TOL. UNLESS OTHERWISE NOTED

Experimental Instrumentation Branch NASA/GSFC Code 924 Greenbelt, Maryland 20771		
Size A	Document Number GLAS/SLA DETECTOR VGA	REV
Date: June 11, 1996	Sheet of	

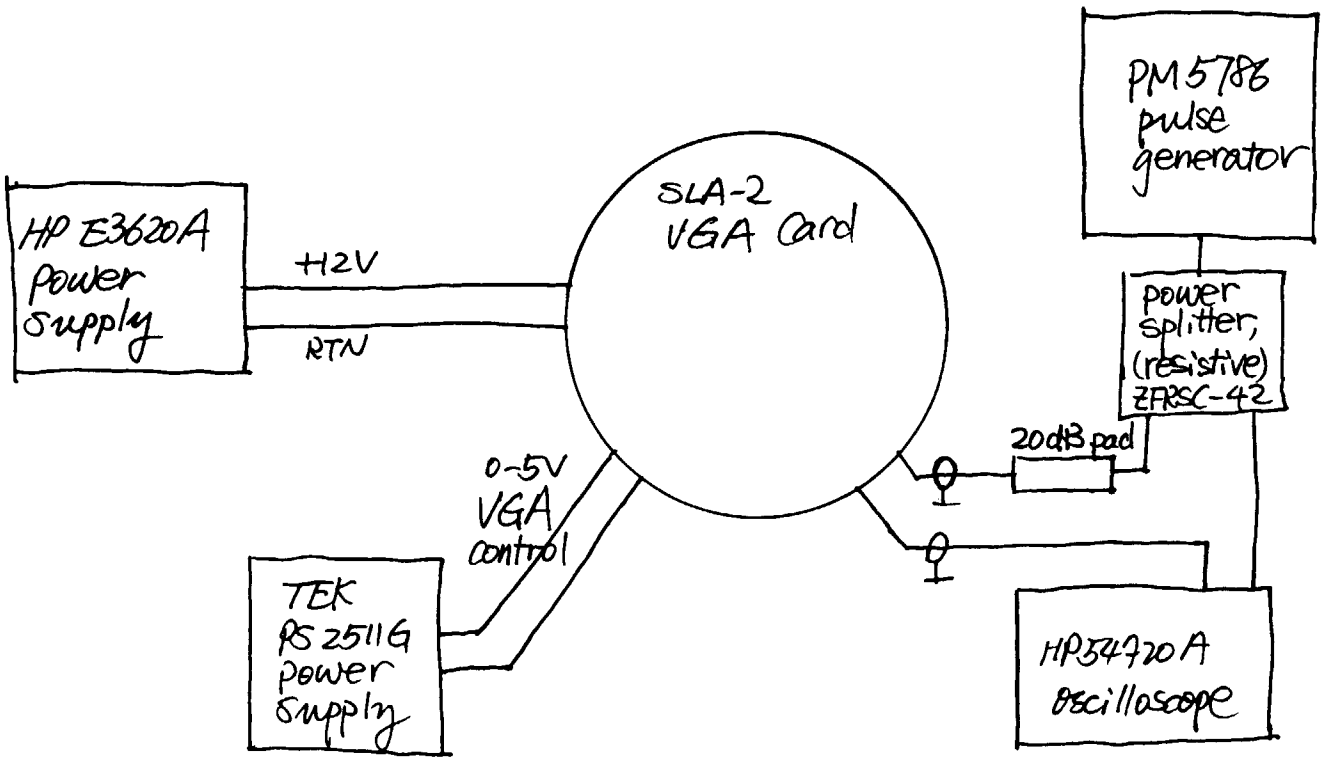

Fig. 2 Test Setup.

VGC volts	n Amp (mV	ut Amp (m	Delay (ns)	Volt Gain	Gain (dB)	Comments
2.89	10.0	172.00	10.79	17.20	24.7	VGC open
0.00	10.0	318.00	10.68	31.80	30.0	
0.55	10.0	317.00	10.70	31.70	30.0	
1.00	10.0	317.00	10.68	31.70	30.0	scope printout
1.50	10.0	317.00	10.70	31.70	30.0	
2.00	10.0	306.00	10.74	30.60	29.7	
2.50	10.0	237.00	10.97	23.70	27.5	
3.00	10.0	150.00	10.68	15.00	23.5	
3.10	10.0	128.00	10.63	12.80	22.1	
3.20	10.0	107.00	10.57	10.70	20.6	
3.24	10.0	99.60	10.54	9.96	20.0	scope printout
3.30	10.0	86.80	10.52	8.68	18.8	
3.40	10.0	67.40	10.49	6.74	16.6	
3.50	10.0	49.00	10.53	4.90	13.8	
3.60	10.0	34.10	10.49	3.41	10.7	
3.70	10.0	22.90	10.43	2.29	7.2	
3.80	10.0	14.20	10.50	1.42	3.0	
3.87	49.9	51.20	10.38	1.03	0.2	scope printout
3.90	49.9	40.10	10.38	0.80	-1.9	
4.00	49.9	26.00	10.35	0.52	-5.7	
4.10	49.9	15.60	10.49	0.31	-10.1	
4.10	200.0	74.70	10.97	0.37	-8.6	slower rising edge (3ns)
4.20	200.0	42.40	11.00	0.21	-13.5	
4.30	200.0	24.30	10.92	0.12	-18.3	
4.33	200.0	20.60	10.88	0.10	-19.7	scope printout
4.40	200.0	14.00	10.80	0.07	-23.1	
4.33	100.0	8.70	10.30	0.09	-21.2	removed the 20dB pad
4.33	300.0	35.10	11.11	0.12	-18.6	
4.33	400.0	39.20	10.89	0.10	-20.2	
4.33	500.0	57.60	11.00	0.12	-18.8	

Fig. 3. Table of test conditions and measurement results.

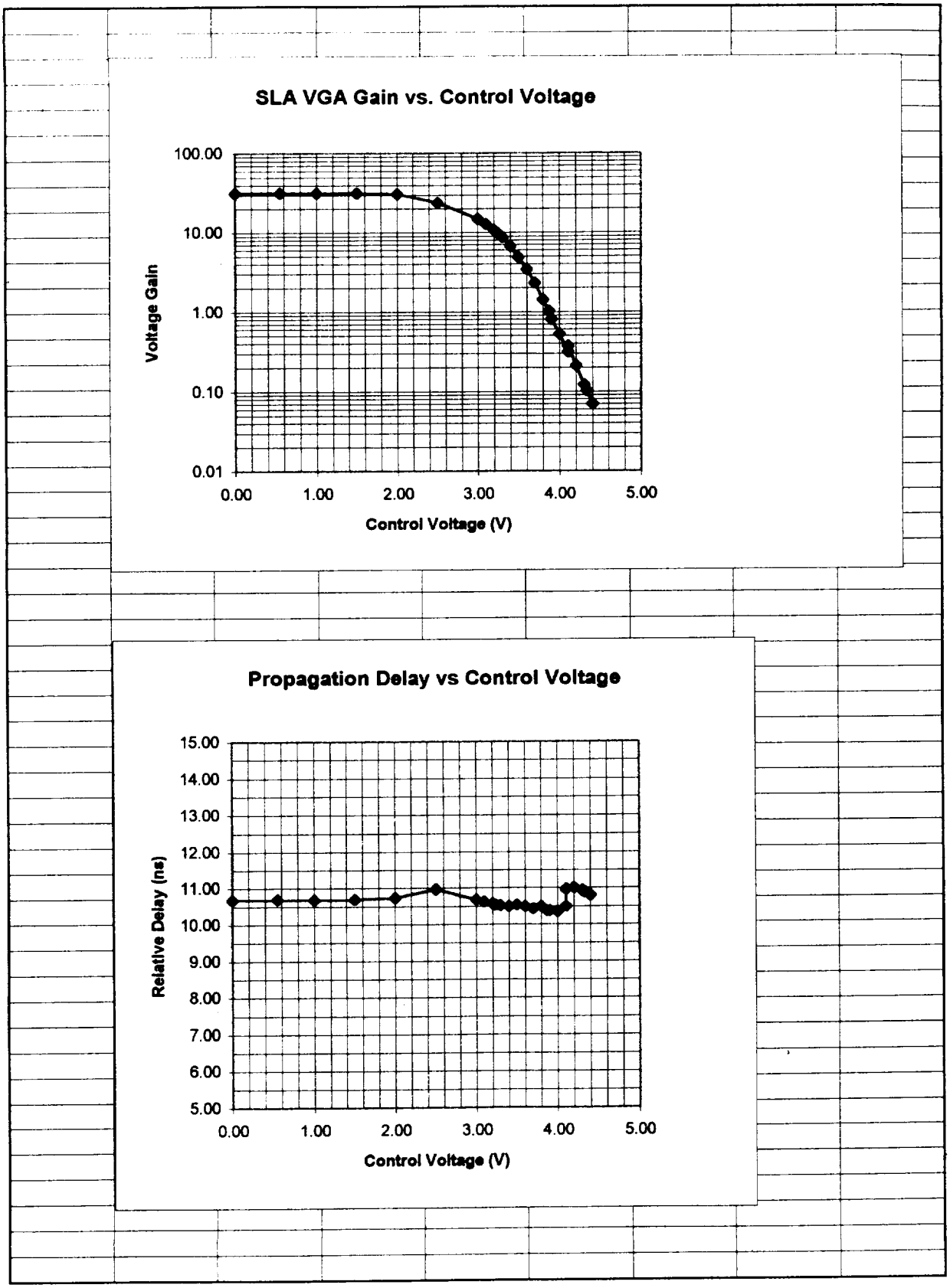

Fig 4. Plots of VGA gain vs. control voltage and relative propagation delay vs. control voltage.

Acquired: 13 JUN 1996 14:02:46.50 Printed: 13 JUN 1996 14:02:46

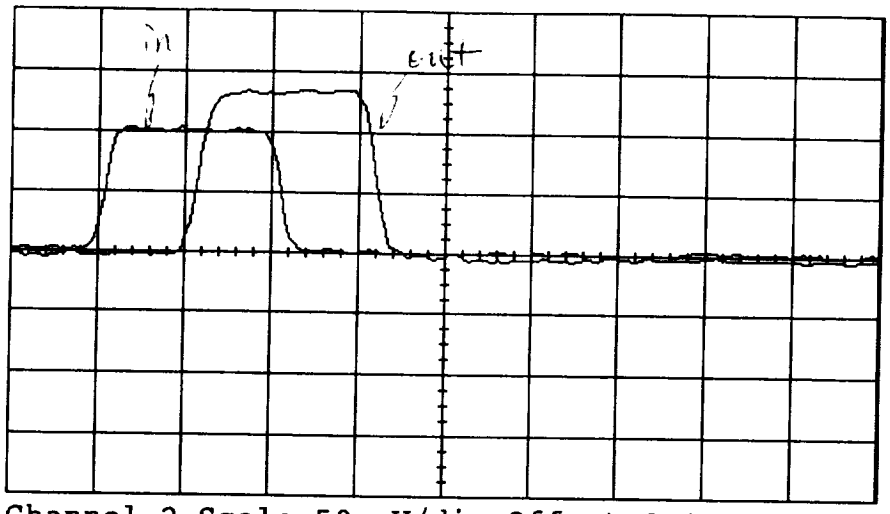

Channel 2 Scale 50 mV/div Offset 0.0 V Input dc 50 Ohms
Channel 3 Scale 100 mV/div Offset 0.0 V Input dc 50 Ohms
Time base Scale 10.0 ns/div Position 38.816 ns Reference center
Trigger Mode edge Source channel 2 Hysteresis normal Holdoff 140 ns
Level 56.0 mV Slope Pos
Measurement

	current	mean	std dev
Risetime(3)	3.27 ns	3.000 ns	133 ps
Falltime(3)	2.73 ns	2.735 ns	144 ps
Risetime(2)	2.24 ns	2.328 ns	102 ps
Falltime(2)	2.30 ns	2.132 ns	116 ps

VGA card output pulse shape at max. gain (close to)

Rise time of the VGA card :

$$\sqrt{3.27^2 - 2.24^2} = 2.4\text{ns}$$

Fig 5. Input and output pulse shape.

Acquired: 13 JUN 1996 12:52:41.60 Printed: 13 JUN 1996 12:52:41

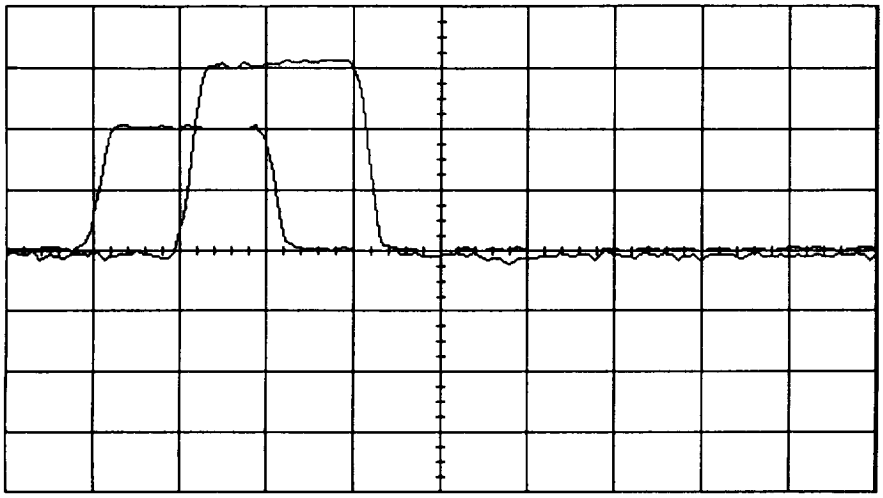

Channel 2 Scale 50 mV/div Offset 0.0 V Input dc 50 Ohms
Channel 3 Scale 100 mV/div Offset 0.0 V Input dc 50 Ohms
Time base Scale 10.0 ns/div Position 38.816 ns Reference center
Trigger Mode edge Source channel 2 Hysteresis normal Holdoff 140 ns
Level 56.0 mV Slope Pos
Measurement

	current	mean	std dev
V amptd(2)	99.1 mV	100.37 mV	740 uV
V amptd(3)	318.2 mV	318.14 mV	3.29 mV
DTime(2)-(3)	10.71 ns	10.689 ns	39 ps

LGC = 1.0 V (max gain)
input = 10 mV

Fig 6. Input and output pulse shape at maximun gain (31.8)

Acquired: 13 JUN 1996 13:09:26.70 Printed: 13 JUN 1996 13:09:26

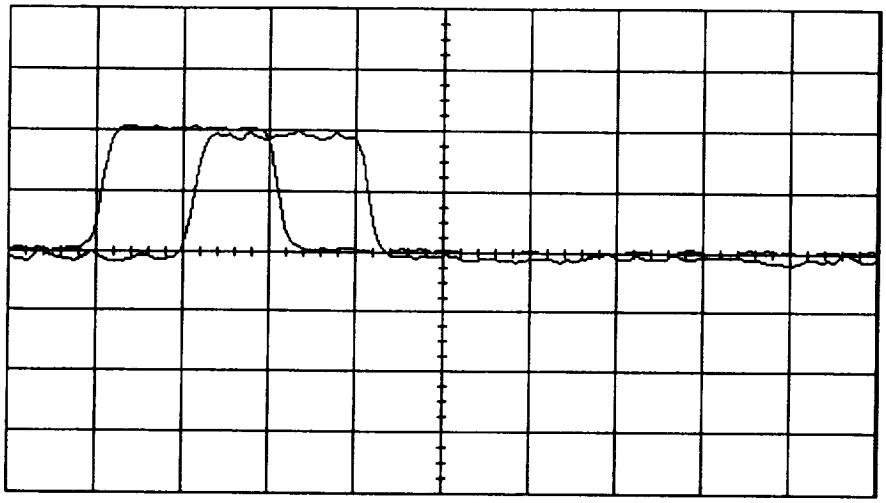

Channel 2 Scale 50 mV/div Offset 0.0 V Input dc 50 Ohms
Channel 3 Scale 50 mV/div Offset 0.0 V Input dc 50 Ohms
Time base Scale 10.0 ns/div Position 38.816 ns Reference center
Trigger Mode edge Source channel 2 Hysteresis normal Holdoff 140 ns
Level 56.0 mV Slope Pos
Measurement

	current	mean	std dev
V amptd(2)	99.9 mV	100.35 mV	710 uV
V amptd(3)	101.1 mV	99.72 mV	1.70 mV
DTime(2)-(3)	10.58 ns	10.544 ns	59 ps

$V_{OC} = 3.24$ V (gain = 10)

input = 10mV

Fig 7. input and output pulse shape at gain of 10.

Acquired: 13 JUN 1996 10:05:41.60 Printed: 13 JUN 1996 10:05:41

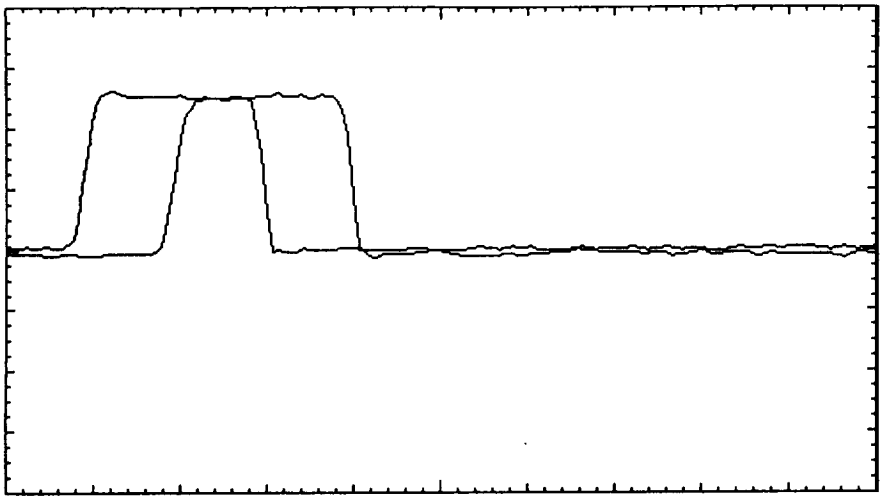

Channel 2 Scale 200 mV/div Offset 0.0 V Input dc 50 Ohms
Channel 3 Scale 20 mV/div Offset 0.0 V Input dc 50 Ohms
Time base Scale 10.0 ns/div Position 41.116 ns Reference center
Trigger Mode edge Source channel 2 Hysteresis normal Holdoff 140 ns
Level 190 mV Slope Pos
Measurement

	current	mean	std dev
V amptd(2)	499 mV	499.46 mV	1.59 mV
V amptd(3)	52.2 mV	51.394 mV	910 uV
DTime(2)-(3)	10.40 ns	10.3849 ns	33.6 ps

$V_{GC} = 3.87$ V (Gain ≃ 1)

input = 50 mV

Fig. 8. Input and output pulseshape at gain of 1.

Acquired: 13 JUN 1996 11:35:51.90 Printed: 13 JUN 1996 11:35:52

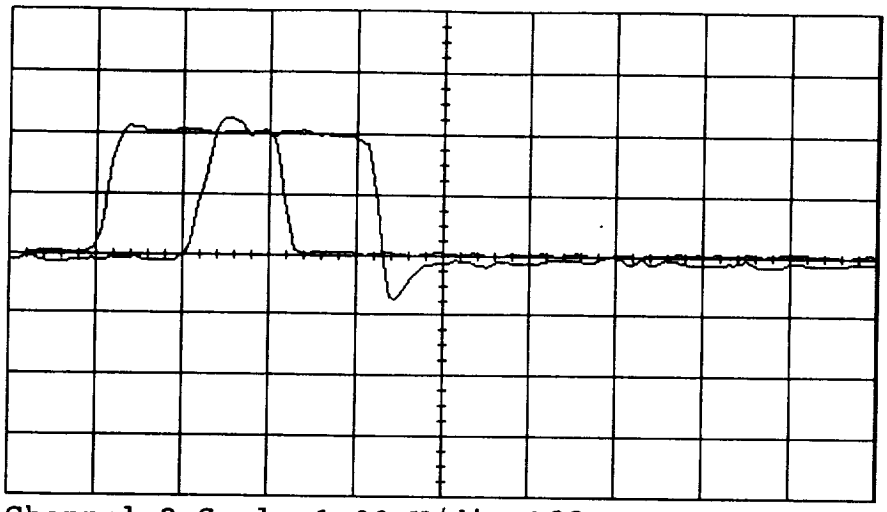

Channel 2 Scale 1.00 V/div Offset 0.0 V Input dc 50 Ohms
Channel 3 Scale 10 mV/div Offset 0.0 V Input dc 50 Ohms
Time base Scale 10.0 ns/div Position 38.816 ns Reference center
Trigger Mode edge Source channel 2 Hysteresis normal Holdoff 140 ns
Level 760 mV Slope Pos
Measurement

	current	mean	std dev
V amptd(2)	1.997 V	2.0018 V	12.7 mV
V amptd(3)	21.42 mV	20.659 mV	398 uV
DTime(2)-(3)	10.82 ns	10.868 ns	61 ps

$V_{GH} = 4.33V$ (gain = 0.10)

input = 200 mV

Fig 9. Input and output pulseshape at gain of 0.10.

Acquired: 14 JUN 1996 10:25:03.30 Printed: 14 JUN 1996 10:25:03

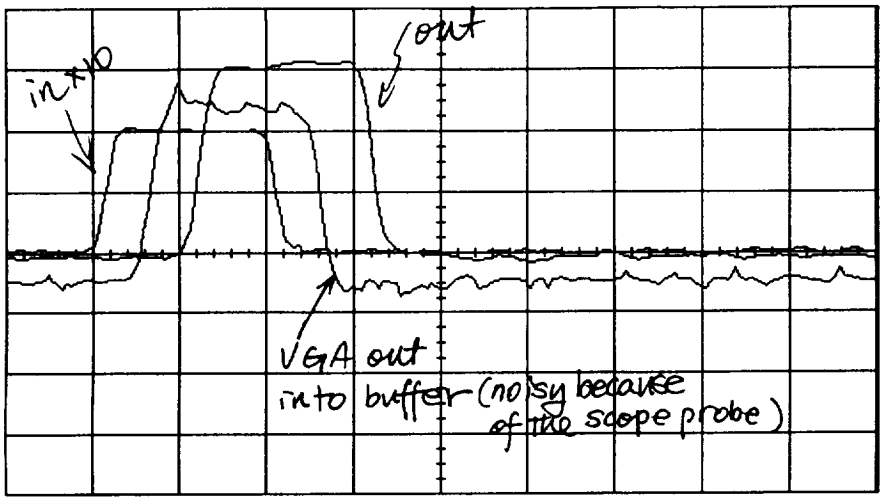

Channel 2 Scale 50 mV/div Offset 0.0 V Input dc 50 Ohms
Channel 3 Scale 100 mV/div Offset 0.0 V Input dc 50 Ohms
Channel 4 Scale 20 mV/div Offset 0.0 V Input ac 1M Ohms
Time base Scale 10.0 ns/div Position 38.500 ns Reference center
Trigger Mode edge Source channel 2 Hysteresis normal Holdoff 140 ns
Level 35.0 mV Slope Pos
Measurement

	current	mean	std dev
V amptd(2)	99.1 mV	99.27 mV	790 uV
V amptd(3)	316.5 mV	312.40 mV	3.73 mV
V amptd(4)	55.2 mV	58.82 mV	4.63 mV

gain of each stage
at max. VGA gain (VGC=1V)

$$\text{VGA gain} = \frac{59\text{mV}}{100\text{mV}/10} = 5.9 = 15.4\,\text{dB}$$

$$\text{Buffer gain} = \frac{312\text{mV}}{59\text{mV}} = 5.29 = 14.5\,\text{dB}$$

Fig 10. input and output pulses at each stage.

Acquired: 14 JUN 1996 10:37:12.70 Printed: 14 JUN 1996 10:37:12

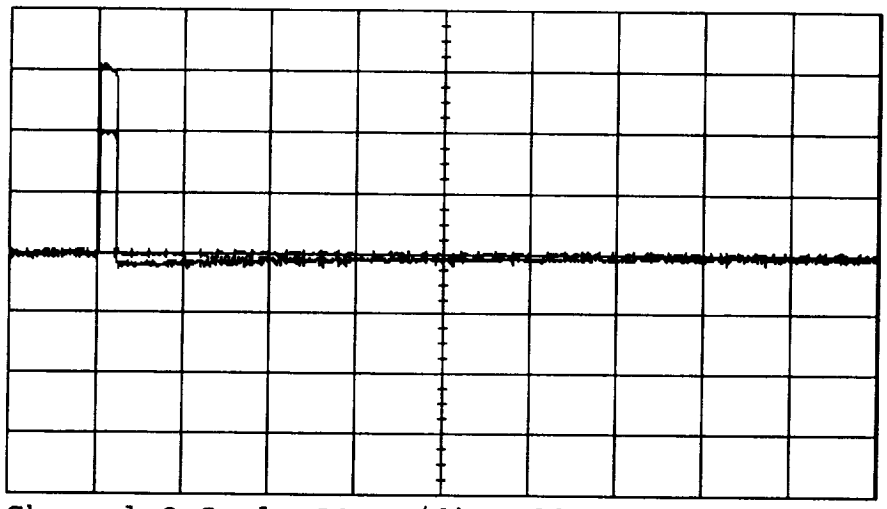

Channel 2 Scale 50 mV/div Offset 0.0 V Input dc 50 Ohms
Channel 3 Scale 100 mV/div Offset 0.0 V Input dc 50 Ohms
Time base Scale 5.00 us/div Position 19.901400 us Reference center
Trigger Mode edge Source channel 2 Hysteresis normal Holdoff 140 ns
Level 35.0 mV Slope Pos
Measurement

	current	mean	std dev
V amptd(2)	99.1 mV	98.39 mV	670 uV
V amptd(3)	313.0 mV	312.16 mV	5.12 mV
V amptd(4)	Source off	----------	----------

input = 1 μs rectangular pulses

output pulse undershoot due to AC coupling at max. gain

Fig. 11. output pulse undershoot due to AC coupling.

Acquired: 14 JUN 1996 07:42:29.90 Printed: 14 JUN 1996 07:43:49

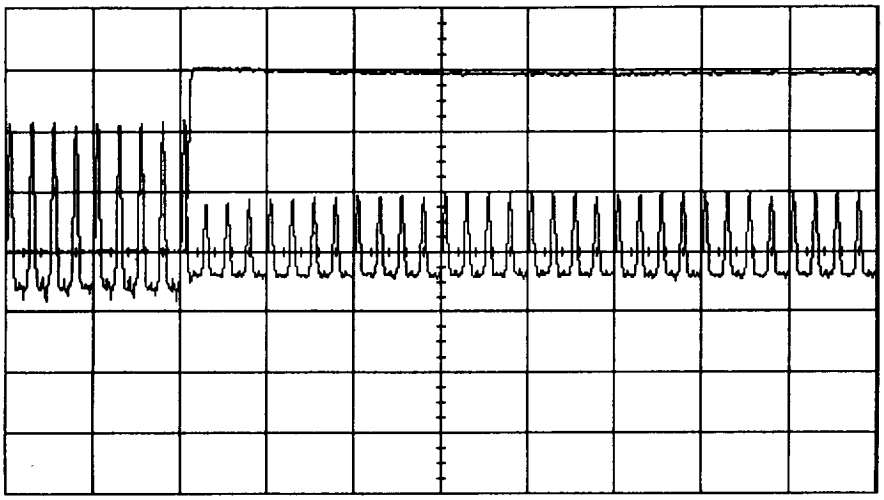

Channel 3 Scale 200 mV/div Offset 0.0 V Input dc 50 Ohms
Channel 4 Scale 1.00 V/div Offset 0.0 V Input dc 1M Ohms
Time base Scale 2.00 us/div Position 5.840000 us Reference center
Trigger Mode edge Source channel 4 Hysteresis normal Holdoff 140 ns
Level 1.02 V Slope Pos

VGA response speed to control

Test setup:

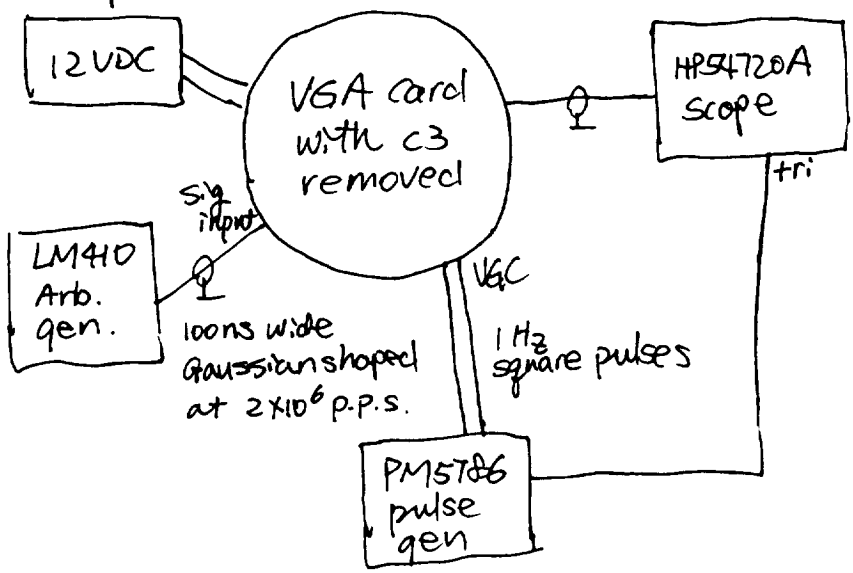

Fig 12. Measurement results of VGA response time.

Acquired: 14 JUN 1996 07:44:46.10 Printed: 14 JUN 1996 07:44:46

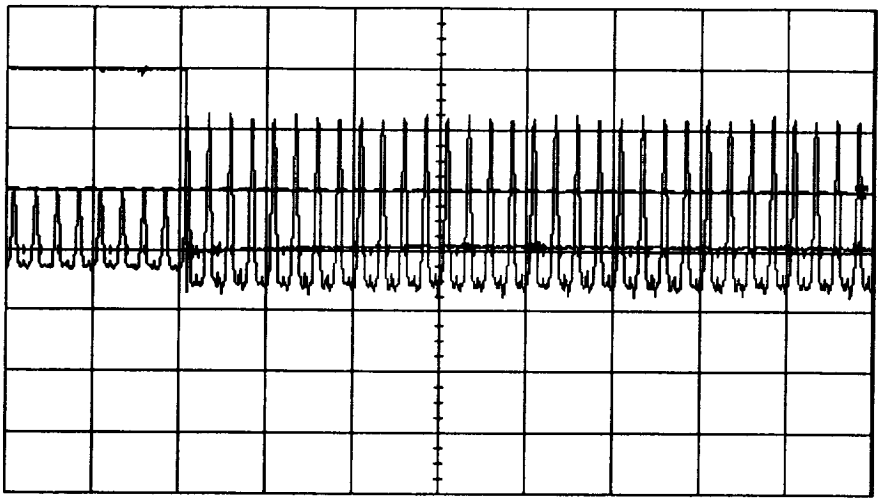

Channel 3 Scale 200 mV/div Offset 0.0 V Input dc 50 Ohms
Channel 4 Scale 1.00 V/div Offset 0.0 V Input dc 1M Ohms
Time base Scale 2.00 us/div Position 5.840000 us Reference center
Trigger Mode edge Source channel 4 Hysteresis normal Holdoff 140 ns
Level 1.02 V Slope Neg

VGA response speed

Fig. 13. Same as Fig. 12 but for VGA gain from low to high.

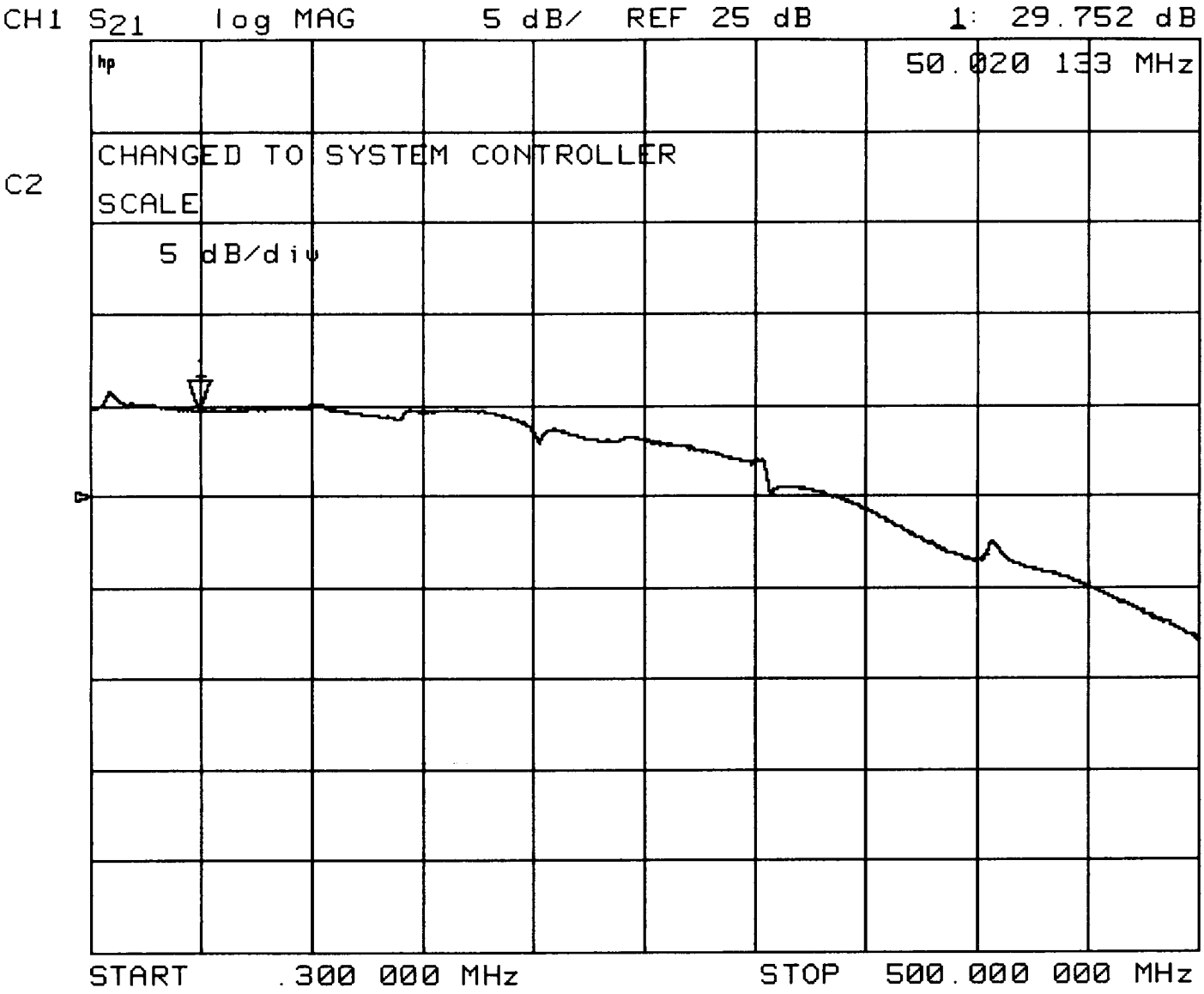

SLA VGA card

The curve shifted down as VGC = 3.6V (Gain ≒ 10dB)

Fig. 14. S_{21}, the S-parameter, measured with HP 8753C/85047 Network analyzer.

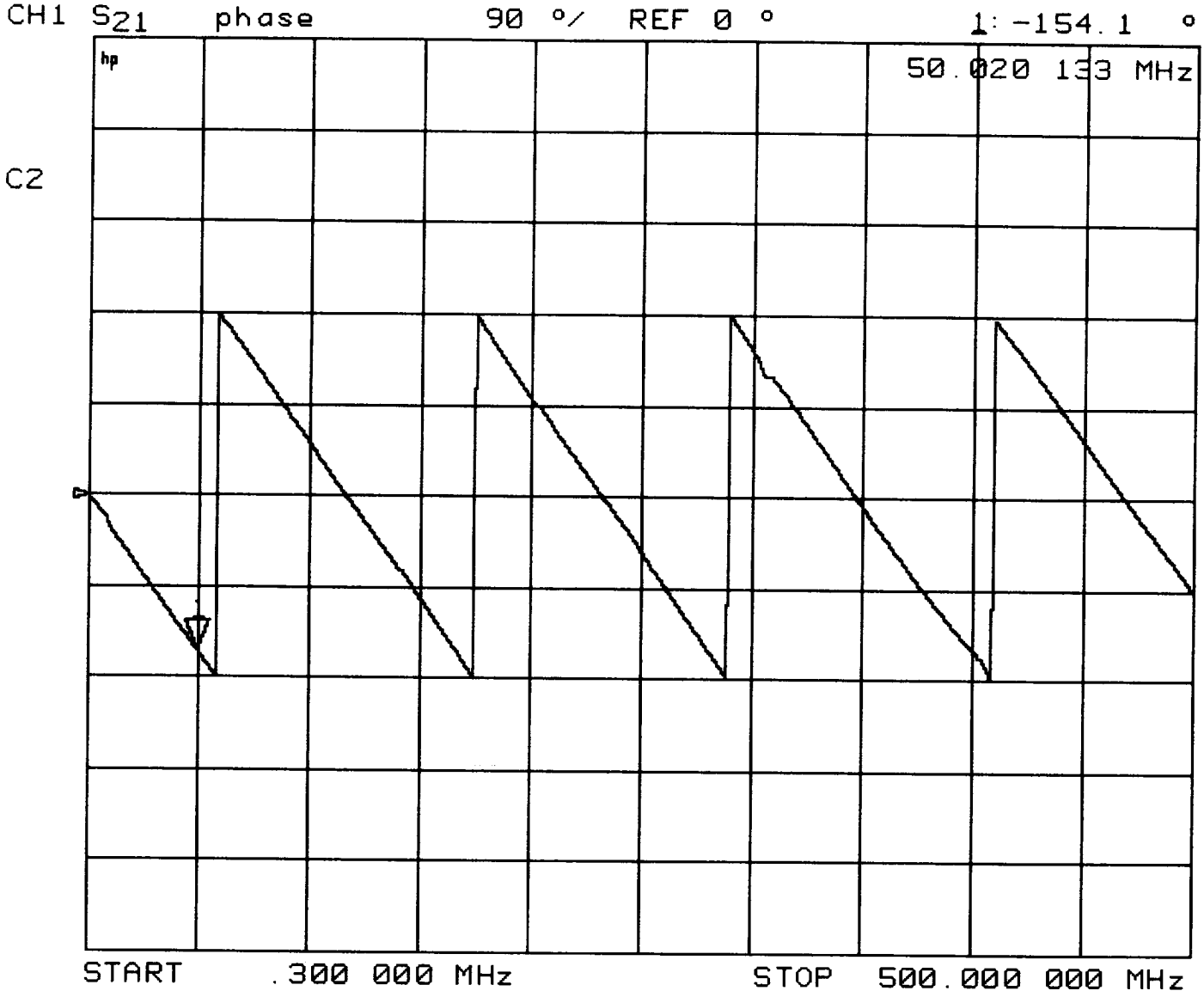

Fig. 15. Same as Fig 14, but the phase.

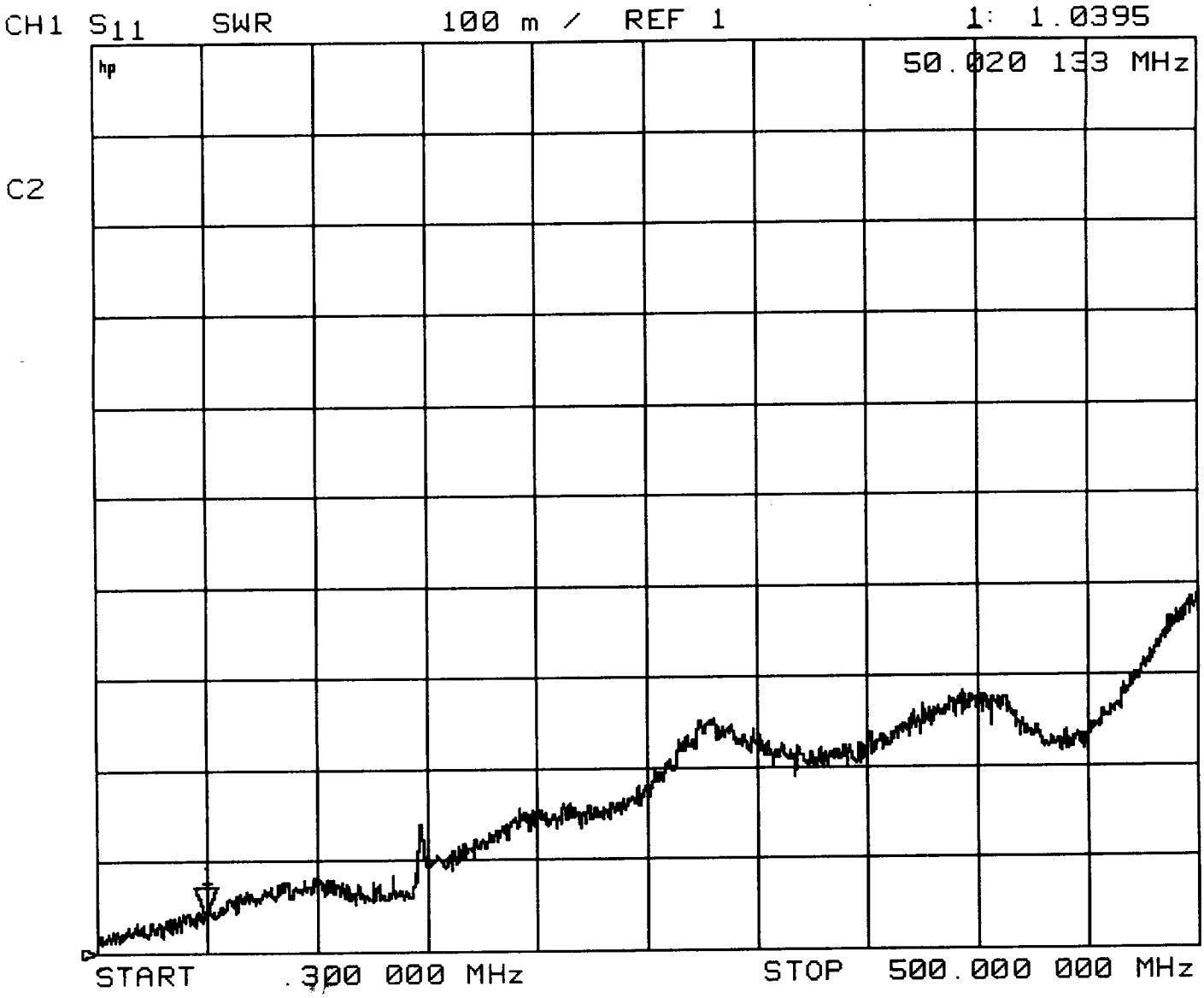

Fig 16. Input VSWR of the VGA card

6-14-96

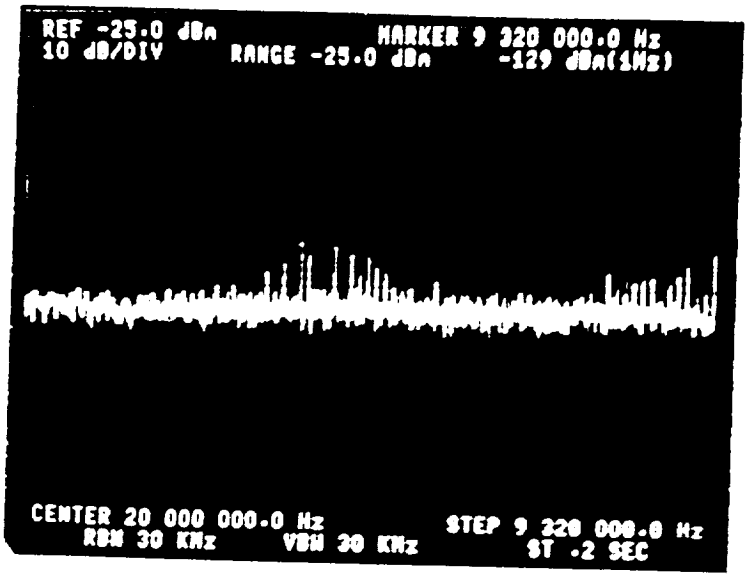

SLA
VGA card
noise spectrum

50Ω term.
at input

20 Hz – 40 MHz

HP3585A

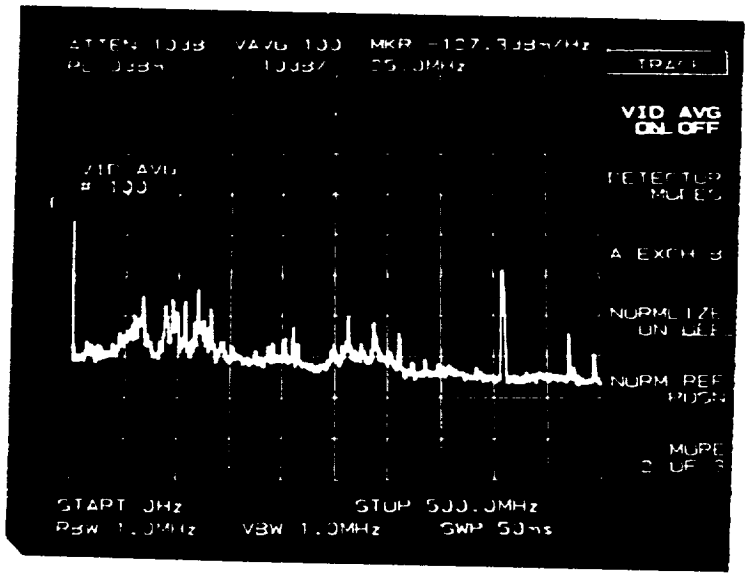

50Ω term
at input

HP 8566B

0 – 500 MHz
(15KHz)

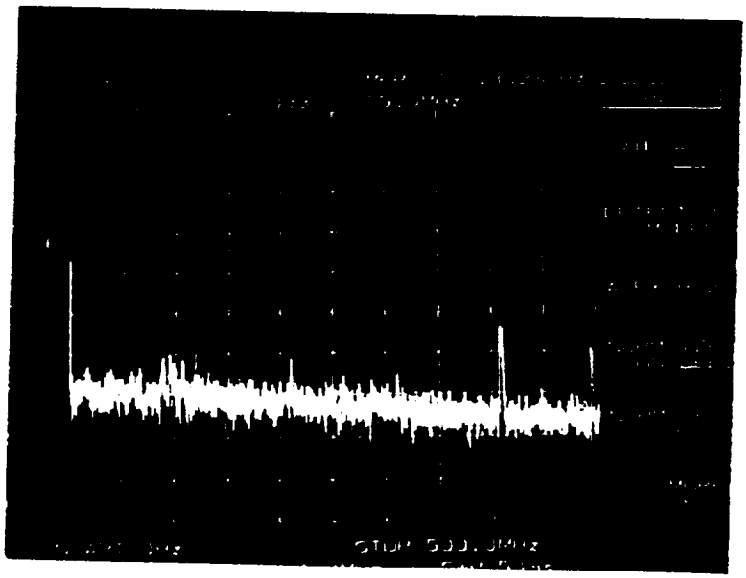

Nothing at input
(cable removed)

Fig. 17 Output noise spectral density of the VGA card.

GLAS Receiver Pulse Width Calculations

slope (rad) rms width at input (ns) laser foot print radius at e^{-2} point (m)

$\alpha := 3 \cdot \frac{2 \cdot \pi}{360}$ $\sigma_t := \frac{5}{2 \cdot \sqrt{2 \cdot \ln(2)}}$ $\sigma_r := 35$

laser pulse shape laser cross section profile speed of light (m/ns)

$f(t) := \frac{1}{\sqrt{2 \cdot \pi} \cdot \sigma_t} \cdot \exp\left(-\frac{t^2}{2 \cdot \sigma_t^2}\right)$ $I(x,y) := \exp\left[-\left(\frac{x^2 + y^2}{\sigma_r^2}\right) \cdot 2\right]$ $c := (3 \cdot 10^8) \cdot 10^{-9}$

$\rho := 2 \cdot \sigma_r$ integration threshold

$$y(t) := \int_0^{\rho} \int_{-\sqrt{\rho^2 - y^2}}^{\sqrt{\rho^2 - y^2}} I(x,y) \cdot f\left(t - \frac{2 \cdot x \cdot \tan(\alpha)}{c}\right) dx\, dy$$

$N := 150$ $\Delta t := 0.5$ $i := 0..N$

$t_i := i \cdot \Delta t - \frac{1}{2} \cdot N \cdot \Delta t$

$Y_i := y(t_i)$ $F_i := f(t_i)$ $Y_{max} := \max(Y)$ $f_{max} := \max(F)$

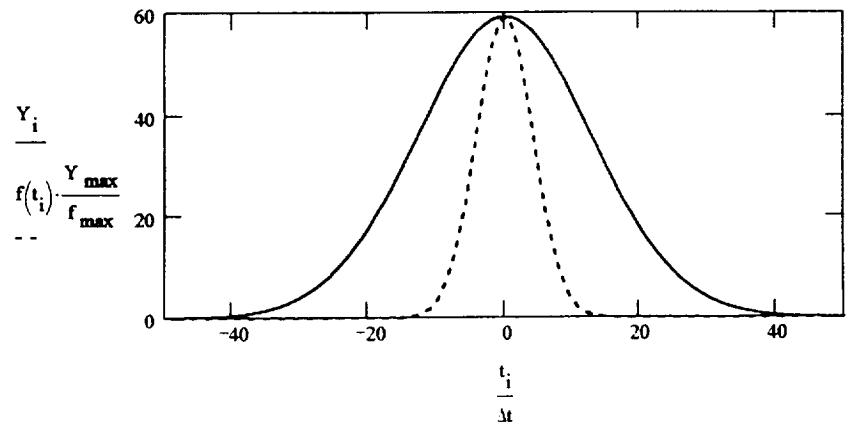

RMS pulsewidth $\sqrt{\left[\sum_i (t_i)^2 \cdot Y_i\right] \cdot \left(\sum_i Y_i\right)^{-1}} = 6.465$

FWHM pulse width

$k := 0..5$ $Z1_k := -F_{k + \frac{N}{2}}$ $\tau 1_k := t_{k + \frac{N}{2}}$ $j := 0..\frac{N}{2}$ $Z2_j := Y_j$ $\tau_j := t_j$

$INFWHM := 2 \cdot \text{linterp}\left(Z1, \tau 1, -\frac{f_{max}}{2}\right)$ $INFWHM = 5$

$OUTFWHM := 2 \cdot \text{linterp}\left(Z2, \tau, \frac{Y_{max}}{2}\right)$ $OUTFWHM = 15.243$

GLAS Receiver Pulse Width Calculations

slope: $\alpha := 0 \cdot \frac{2 \cdot \pi}{360}$

rms width at input (ns): $\sigma_t := \frac{5}{2 \cdot \sqrt{2 \cdot \ln(2)}}$

laser foot print radius (m): $\sigma_r := 35$

$$f(t) := \frac{1}{\sqrt{2 \cdot \pi} \cdot \sigma_t} \cdot \exp\left(-\frac{t^2}{2 \cdot \sigma_t^2}\right)$$

$c := (3 \cdot 10^8) \cdot 10^{-9}$

$\rho := 2 \cdot \sigma_r$ $TOL := 10^{-5}$

$$y(t) := \int_{-\rho}^{\rho} \exp\left[-\left(\frac{x^2}{\sigma_r^2}\right) \cdot 2\right] \cdot f\left(t - \frac{2 \cdot x \cdot \tan(\alpha)}{c}\right) \cdot \operatorname{erf}\left(\sqrt{\rho^2 - x^2} \cdot \frac{2}{\sigma_r}\right) dx$$

$N := 100$ $\Delta t := .1$ $i := 0..N$

$t_i := i \cdot \Delta t - \frac{N}{1} \cdot \Delta t$

$Y_i := y(t_i)$ $F_i := f(t_i)$ $Y_{max} := \max(Y)$ $f_{max} := \max(F)$

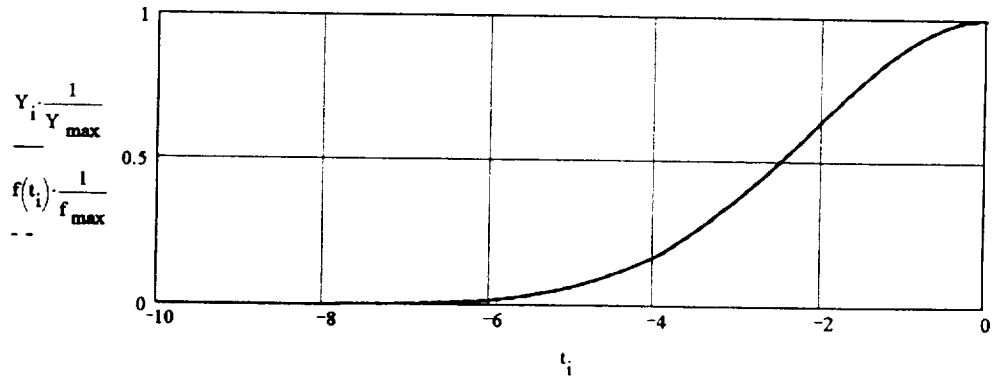

RMS pulsewidth $\sqrt{\left[\sum_i (t_i)^2 \cdot Y_i\right] \cdot \left(\sum_i Y_i\right)^{-1}} = 2.104$

FWHM pulse width

$k := 0..100$ $Z1_k := -F_{N-k}$ $\tau 1_k := t_{N-k}$ $j := 0..(N-10)$ $Z2_j := -Y_{N-j}$ $\tau_j := t_{N-j}$

$INFWHM := 2 \cdot \left| \text{linterp}\left(Z1, \tau 1, -\frac{f_{max}}{2}\right) \right|$ $INFWHM = 5$

$OUTFWHM := 2 \cdot \left| \text{linterp}\left(Z2, \tau, \frac{-Y_{max}}{2}\right) \right|$ $OUTFWHM = 5$

GLAS Receiver Pulse Width Calculations

slope rms width at input (ns) laser foot print radius (m)

$\alpha := 40 \cdot \frac{2 \cdot \pi}{360}$ $\sigma_t := \frac{5}{2 \cdot \sqrt{2 \cdot \ln(2)}}$ $\sigma_r := 35$

$\rho := 2 \cdot \sigma_r$ $c := (3 \cdot 10^8) \cdot 10^{-9}$

$$y(t,\alpha) := \begin{cases} \left[\exp\left[-\left[\frac{\left(\frac{c \cdot t}{2 \cdot \tan(\alpha)}\right)^2}{\sigma_r^2}\right] \cdot 2\right] \cdot \operatorname{erf}\left[\sqrt{\rho^2 - \left(\frac{c \cdot t}{2 \cdot \tan(\alpha)}\right)^2} \cdot \frac{2}{\sigma_r}\right]\right] & \text{if } \left|\frac{c \cdot t}{2 \cdot \tan(\alpha)}\right| \le \rho \\ 0 \quad \text{otherwise} \end{cases}$$

$N := 150$ $\Delta t := 3$ $i := 0..N$

$t_i := i \cdot \Delta t - \frac{N}{1} \Delta t$ $Y_i := y(t_i, \alpha)$ $Y_{max} := \max(Y)$

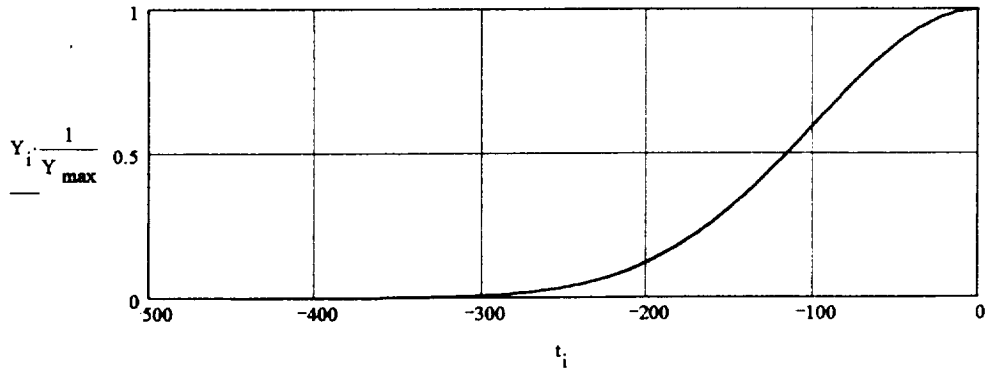

RMS pulsewidth $\sqrt{\left[\sum_i (t_i)^2 \cdot Y_i\right] \cdot \left(\sum_i Y_i\right)^{-1}} = 97.231$ 40° 137.5 50° 201.172 60° 319.705 70°

FWHM pulse width

$j := 0..(N - 80)$ $Z2_j := -Y_{N-j}$ $\tau_j := t_{N-j}$

$OUTFWHM := 2 \cdot \left|\text{linterp}\left(Z2, \tau, \frac{-Y_{max}}{2}\right)\right|$ $OUTFWHM = 230.532$ 40° 327.414 52° 475.43 60° 751.515 70°

GLAS Received Laser Pulse Width vs Ground Slope

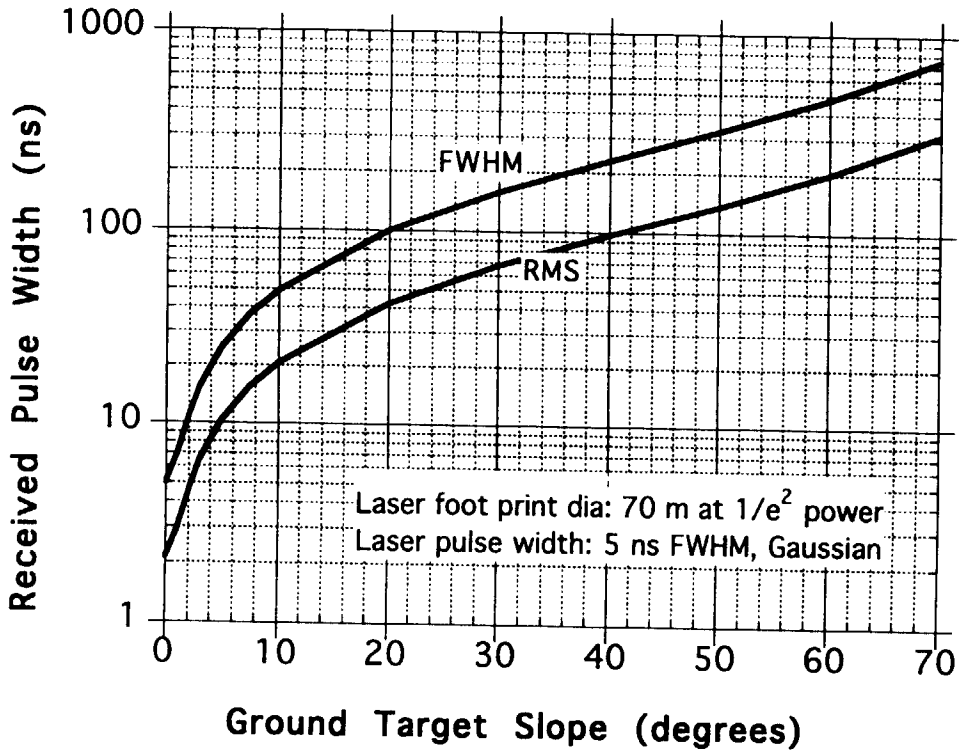

GLAS Altimeter Link Margin Analysis

Xiaoli Sun, The Johns Hopkins University

System parameters

$E_t := 0.0740$	Laser transmitter pulse energy (J)
$R := 598 \cdot 10^3$	Range to the target (m)
$r_{diff} := 0.60$	Target diffusion coefficient
$\phi_{tel} := 0.90$	Receiver Telescope Diameter (m)
$\phi_{obs} := 0.25$	Telescope center obscuration (m)
$\eta_{rcvr} := 0.5$	Receiver optics transmission
$\theta_{FOV} := 0.30 \cdot 10^{-3}$	Receiver FOV, full angle (rad)
$\Delta\lambda := 0.60 \cdot 10^{-3}$	Receiver optical bandwidth (um)
$\eta_{atmo} := 0.5$	Atmosphere Transmission Coefficient (one way)
$I_{solar} := 720$	Solar irradiance at the target (W/m^2/um)

Other system parameter values:

$\tau := 15.242 \cdot 10^{-9}$	Received laser pulse width (receiver integration time) (s)
$\eta_{APD} := 0.35$	APD quantum efficiency
$G := 150$	Average APD gain
$k_{eff} := 0.01$	APD ionization coefficient ratio
$I_b := 50 \cdot 10^{-12}$	APD bulk leakage current (A)
$I_s := 15 \cdot 10^{-9}$	APD surface leakage current (A)
$N_{amp} := \left(2.6 \cdot 10^{-12}\right)^2$	Preamp spectral noise current density (A^2/Hz)
$BW_n := \frac{2.204}{2 \cdot \pi \cdot \tau}$	Receiver noise bandwidth (Hz) $BW_n = 2.3014 \cdot 10^7$
$R_G := 20 \cdot 10^3$	Range gate (km)

RECEIVED SIGNAL AND NOISE

Solar background noise photons per second

$$P_b := I_{solar}\cdot\Delta\lambda\cdot\eta_{rcvr}\cdot\pi\cdot\left(\frac{\theta_{FOV}}{2}\right)^2\cdot\frac{r_{diff}}{\pi}\cdot\left(\pi\cdot\frac{\phi_{tel}^{\ 2}-\phi_{obs}^{\ 2}}{4}\right)$$

$$\lambda_b := \frac{\eta_{APD}\cdot P_b}{1.17\cdot 1.6\cdot 10^{-19}} \qquad n_b := \lambda_b\cdot\tau$$

Telescope area $\left(\pi\cdot\frac{\phi_{tel}^{\ 2}-\phi_{obs}^{\ 2}}{4}\right) = 0.5871$

$P_b = 1.7119\cdot 10^{-9}$ $\qquad n_b = 48.79$

Received signal pulse energy

$$E_r := E_t\cdot\frac{r_{diff}}{\pi}\cdot\left(\pi\cdot\frac{\phi_{tel}^{\ 2}-\phi_{obs}^{\ 2}}{4\cdot R^2}\right)\cdot\eta_{rcvr}\cdot\eta_{atmo}^{\ 2} \qquad E_r\cdot 10^{15} = 2.9003$$

Signal photons per received pulse

$$N_s := \frac{E_r}{1.17\cdot 1.6\cdot 10^{-19}} \qquad N_s = 1.5493\cdot 10^4 \qquad N_s\cdot\eta_{APD} = 5.4226\cdot 10^3$$

PROBABILITY OF MISSES AND FALSE ALARM

The means of the APD outputs:

noise only $\qquad \mu_0 := \left(n_b + \frac{I_b}{1.6\cdot 10^{-19}}\cdot\tau\right) \qquad \mu_0 = 53.5488$

signal and noise $\qquad \mu_1(n_s) := n_s + \mu_0$

The variance of the preamplifier noise and APD surface leakage current noise:

$$var := \left[\frac{N_{amp}\cdot\tau}{\left(1.6\cdot 10^{-19}\right)^2} + \frac{I_s\cdot\tau}{1.6\cdot 10^{-19}}\right] \qquad \sigma := \sqrt{var} \qquad \frac{var}{G^2} = 1.7895\cdot 10^2$$

Noise contributions from the preamp noise and APD surface leak current

$$\sqrt{\frac{N_{amp}\cdot\tau}{\left(1.6\cdot 10^{-19}\right)^2}}\cdot\frac{1}{G} = 13.3747 \qquad \sqrt{\frac{I_s\cdot\tau}{1.6\cdot 10^{-19}}}\cdot\frac{1}{G} = 0.252$$

The p.d.f. of the APD output using Webb's approximation:

APD excess noise factor

$$F := k_{eff} \cdot G + \left(2 - \frac{1}{G}\right) \cdot \left(1 - k_{eff}\right) \qquad F = 3.4734$$

signal absent, noise only

$$s_{00} := \sqrt{G^2 \cdot F \cdot \mu_0} \qquad s_{00} = 2.0457 \cdot 10^3$$

$$P_{PD0}(z) := \frac{1}{\sqrt{2 \cdot \pi}} \cdot \frac{1}{\left[1 + \frac{G \cdot (F-1) \cdot z}{s_{00}}\right]^{\frac{3}{2}}} \cdot \exp\left[\frac{-z^2}{2 \cdot \left[1 + \frac{G \cdot (F-1) \cdot z}{s_{00}}\right]}\right]$$

signal plus noise

$$s_{11}(n_s) := \sqrt{G^2 \cdot F \cdot \mu_1(n_s)}$$

$$P_{PD1}(z, n_s) := \frac{1}{\sqrt{2 \cdot \pi}} \cdot \frac{1}{\left[1 + \frac{G \cdot (F-1) \cdot z}{s_{11}(n_s)}\right]^{\frac{3}{2}}} \cdot \exp\left[\frac{-z^2}{2 \cdot \left[1 + \frac{G \cdot (F-1) \cdot z}{s_{11}(n_s)}\right]}\right]$$

Probabilities of false alarm:

Calculate the integration upper and lower limits

lower limit of the integral $z_0 := \frac{-G \cdot \mu_0}{s_{00}}$

Upper limit of the integral $z_1 := 100$

Standard deviation of the total noise

$$s_0 := \sqrt{s_{00}^2 + \sigma^2} \qquad s_0 = 2.8655 \cdot 10^3$$

$$p_{fa}(n_T) := \int_{z_0}^{z_1} P_{PD0}(z) \cdot cnorm\left(\frac{s_{00} \cdot z - n_T \cdot s_0}{\sigma}\right) dz$$

The built-in function "cnorm(u)" is the cumulative probability distribution function of a Gaussian r.v. with zero mean and unity variance

Range gate interval (sec) $T := 2 \cdot \frac{R_G \cdot 1000}{3 \cdot 10^8}$ $T = 0.1333$

$$P_{FA}(n_T) := 1 - \exp\left(-\frac{T}{\tau} \cdot p_{fa}(n_T)\right)$$

The probability of correct detection:

upper and lower limits of the integral

$z_{11} := 100$ $z_{01}(n_s) := \frac{-G \cdot \mu_1(n_s)}{s_{11}(n_s)}$

$$P_D(n_s, n_T) := \int_{z_{01}(n_s)}^{z_{11}} P_{PD1}(z, n_s) \cdot cnorm\left[\frac{s_{11}(n_s) \cdot z - n_T \cdot s_0 + G \cdot (\mu_1(n_s) - \mu_0)}{\sigma}\right] dz$$

Solution for the normalized threshold level at a given false alarm rate

$M := 10$ $k := 0, 1 .. M$ $TOL := 10^{-12}$ The integration error tolerance

$NT_k := 6.5 + 0.25 \cdot k$ Normalized threshold level wrt to the standard deviation of the total noise

$pfa_k := p_{fa}(NT_k)$ $PFA_k := 1 - \exp\left(-\frac{T}{\tau} \cdot pfa_k\right)$

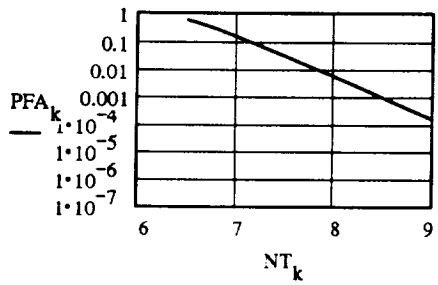

Find the point at PFA=0.01

$PPFA_k := PFA_{M-k}$

$NNT_k := NT_{M-k}$

$Th_{opt} := linterp(PPFA, NNT, 0.01)$

$Th_{opt} = 7.8443$

The link margin calculation:

$N := 10$ $i := 0..N$ $TOL := 10^{-5}$

$ns_i := 0.015 + i \cdot \frac{.025}{N}$ normalized signal level

$PD_i := P_D\left(ns_i \cdot N_s \cdot \eta_{APD}, Th_{opt}\right)$

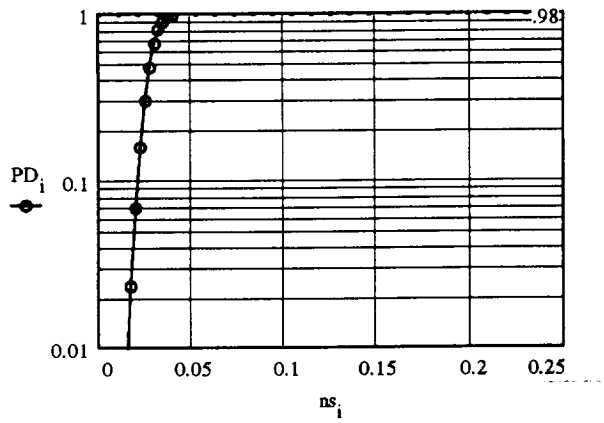

$$ns = \begin{bmatrix} 0.015 \\ 0.0175 \\ 0.02 \\ 0.0225 \\ 0.025 \\ 0.0275 \\ 0.03 \\ 0.0325 \\ 0.035 \\ 0.0375 \\ 0.04 \end{bmatrix} \quad PD = \begin{bmatrix} 6.2341 \cdot 10^{-3} \\ 0.0237 \\ 0.069 \\ 0.1597 \\ 0.3012 \\ 0.477 \\ 0.6535 \\ 0.7988 \\ 0.898 \\ 0.9549 \\ 0.9826 \end{bmatrix}$$

Signal level at PD*(1-PFA)<=0.98

$PPD(x) := linterp(ns, PD, x)$ form a function of PD vs. normalized threshold

$x_g := 0.013$ initial guess

$sig_{min} := root\left(PPD\left(x_g\right) - \frac{0.98}{1 - 0.01}, x_g\right)$

Link margin:

$sig_{min} = 0.0407$ $10 \cdot \log\left(\frac{1}{sig_{min}}\right) = 13.9085$ (dB)

Link margin vs. transmitted laser pulse energy

$l := 1..20$

$sig_l := 0.05 \cdot l$ $SIG_l := sig_l \cdot E_t$

$LM1_l := 10 \cdot \log\left(\frac{sig_l}{sig_{min}}\right)$

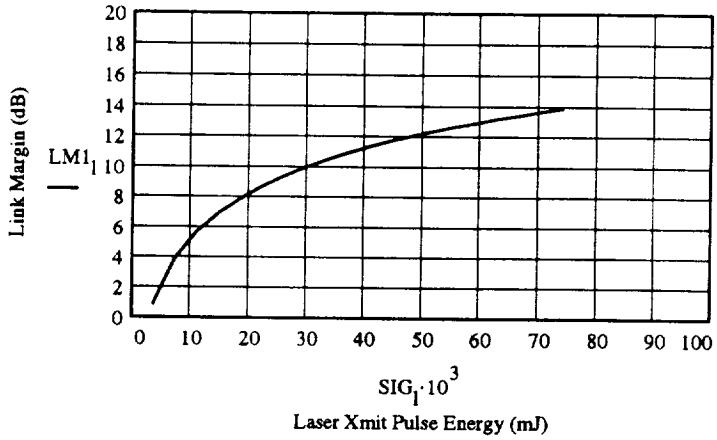

Link margin vs. received pulse width:

$k := 1, 2 .. 80$

$TFWHM_k := k \cdot 20 \cdot 10^{-9}$

Actual received signal vs. received pulse width

(Here the receiver was approximated as an integrator, since the distribution of a filtered APD output is too difficult to model at this time.)

$$smax_k := if\left(TFWHM_k \le \tau, 1, \frac{\tau}{TFWHM_k}\right)$$

$$LM2_k := 10 \cdot \log\left(\frac{smax_k}{sig_{min}}\right)$$

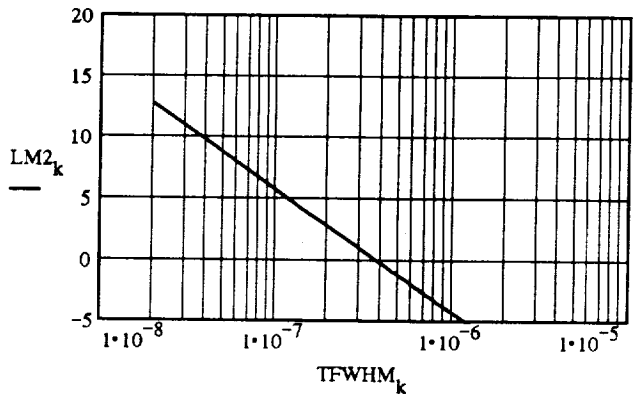

Link Margin vs. One-way Atmosphere Transmission

minimun detectable signal if transmission=100%: $sig0_{min} := sig_{min} \cdot (\eta_{atmo})^2$

$M := 30 \qquad m := 1..M$

$TATMO_m := \frac{m}{M}$

$LM3_m := 10 \cdot \log\left[\frac{(TATMO_m)^2}{sig0_{min}}\right]$

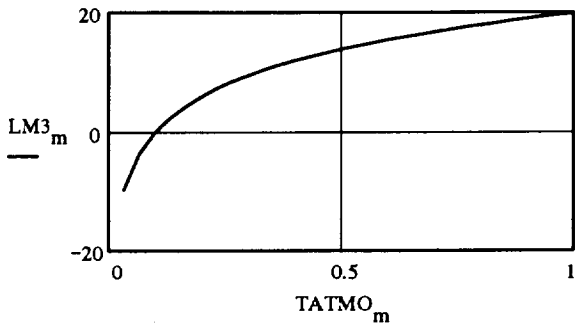

WRITEPRN(LMvsEt) := augment(SIG, LM1)

WRITEPRN(LMvsFWHM) := augment(TFWHM, LM2)

WRITEPRN(LMvsTATMO) := augment(TATMO, LM3)

Notes to the Mathcad Program for Laser Altimeter Link Analysis

Xiaoli Sun, Code 924/JHU, May 18, 1995

1. False Alarm Probability

The average rate of false alarms can be calculated as[1]

$$T_{FA}^{-1}=\frac{p_{fa}}{\tau_W} \tag{1}$$

where p_{fa} is the false alarm probability at a fixed time and τ_W is the average noise pulse width above the threshold. It may be assumed that $\tau_W=1/BW_{3dB}$. The number of false alarms over a given range gate time, T_G, follows a Poisson distribution and the false alarm probability is given by

$$P_{FA}=1-\exp\left[-\frac{T_G}{T_{FA}}\right]=1-\exp[-T_G BW_{3dB} p_{fa}] \tag{2}$$

The false alarm probability at a fixed time can be written as

$$p_{fa}=\int_{y_T}^{\infty} p(y|\mu_0)dy=\int_{y_T}^{\infty}\int_{0}^{\infty}\frac{1}{\sqrt{2\pi}\sigma}\exp\left[-\frac{(y-x-\mu_g)^2}{2\sigma^2}\right]P_{PD}(x|\mu_0)dxdy \tag{3}$$

where $p(y|\mu_0)$ is the p.d.f. of the APD preamplifier output and is equal to the convolution of the p.d.f. of the APD output and the p.d.f. of the preamplifier noise. The latter is assumed to be additive and Gaussian with mean, μ_g, and standard deviation, σ. Usually, the preamplifier itself has zero DC offset, $\mu_g=I_s\tau/q$ with I_s the APD surface leakage current, τ the equivalent integration time of the lowpass filter, and q the electron charge. The variance is given by

$$\sigma^2=(N_{amp}+2I_s)BW_n\tau^2/q^2 \tag{4}$$

with N_{amp} the one sided input noise spectral density of the preamplifier in (A^2/Hz) and BW_n the noise bandwidth of the lowpass filter.

The p.d.f. of the APD output in number of photoelectrons is given by[2]

---

[1] M. I. Skolnik, Introduction to Radar Systems, McGraw-Hill, New York, 1962, p. 31.

[2] P. P. Webb, R. J. McIntyre, and J. Conradi, "Property of avalanche photodiodes," *RCA Review*, Vol. 35, pp. 234-278, June 1974.

$$P_{PD}(x|\mu_0)=\frac{1}{\sqrt{2\pi G^2F\mu_0}}\frac{1}{\left[1+\frac{(x-G\mu_0)(F-1)}{GF\mu_0}\right]^{3/2}}\exp\left\{\frac{-(x-G\mu_0)^2}{2G^2F\mu_0\left[1+\frac{(x-G\mu_0)(F-1)}{GF\mu_0}\right]}\right\} \quad (5)$$

where μ_0 is the average number of primary photoelectrons given by

$$\mu_0=\frac{\eta_{APD}P_b\tau}{hf}+\frac{I_b\tau}{q} \quad (6)$$

with η_{APD} the APD quantum efficiency, P_b the received background noise power, hf the photon energy, and I_b the APD bulk leakage current.

Interchange the order of integrations in Eq. (3) and substitute $u=(x-y+\mu_g)/\sigma$, and $z=(x-G\mu_0)/(G^2F\mu_0)^{1/2}$,

$$p_{fa}=\int_0^\infty\left\{\int_{y_T}^\infty\frac{1}{\sqrt{2\pi}\sigma}\exp\left[-\frac{(y-x-\mu_g)^2}{2\sigma^2}\right]dy\right\}P_{PD}(x|\mu_0)dx$$

$$=\int_0^\infty\left\{\int_{-\infty}^{\frac{x-y_T+\mu_g}{\sigma}}\frac{1}{\sqrt{2\pi}}\exp\left[-\frac{u^2}{2}\right]du\right\}P_{PD}(x|\mu_0)dx$$

$$=\int_{\frac{-G\mu_0}{\sqrt{G^2F\mu_0}}}^\infty\Phi\left[\frac{\sqrt{G^2F\mu_0}\,z-(y_T-G\mu_0-\mu_g)}{\sigma}\right]P_{PDZ}(z|\mu_0)dz \quad (7)$$

$$\Phi[x]=\int_{-\infty}^{x}\frac{1}{\sqrt{2\pi}}\exp\left[-\frac{u^2}{2}\right]du \quad (8)$$

$$P_{PDZ}(z|\mu_0)=\frac{1}{\sqrt{2\pi}}\frac{1}{\left[1+\frac{G(F-1)z}{\sqrt{G^2F\mu_0}}\right]^{3/2}}\exp\left\{\frac{-z^2}{2\left[1+\frac{G(F-1)z}{\sqrt{G^2F\mu_0}}\right]}\right\} \quad (9)$$

A normalized threshold is defined as

$$Y_T=\frac{y_T-(G\mu_0+\mu_g)}{\sqrt{G^2F\mu_0+\sigma^2}} \quad (10)$$

that is, Y_T is how many standard deviations the actual threshold is above the average DC component. Usually, $\mu_g<<G\mu_0$, we can drop μ_g in the calculations.

Substitute (10) into (7)

$$P_{fa}=\int_{\frac{-G\mu_0}{\sqrt{G^2F\mu_0}}}^{\infty}\Phi\left[\frac{\sqrt{G^2F\mu_0}\,z-Y_T\sqrt{G^2F\mu_0+\sigma^2}}{\sigma}\right]P_{PDZ}(z|\mu_0)dz \qquad (11)$$

2. Probability of Correct Detection

The probability of correction detection can be written as

$$P_D=\int_{Y_T}^{\infty}p(x|\mu_1)dx=\int_{Y_T}^{\infty}\int_{0}^{\infty}\frac{1}{\sqrt{2\pi}\sigma}\exp\left[-\frac{(y-x)^2}{2\sigma^2}\right]P_{PD}(x|\mu_1)dxdy \qquad (12)$$

where μ_1 is the average number primary photoelectrons when the signal is present,

$$\mu_1=\mu_0+n_s \qquad (13)$$

with n_s the average number of detected signal photons per pulse.

Similar to (7), interchange the order of integrations in Eq. (12) and substitute $u=(x+\mu_g-y)/\sigma$, and $z=(x-G\mu_1)/(G^2F\mu_1)^{1/2}$,

$$\begin{aligned}P_D&=\int_{\frac{-G\mu_1}{\sqrt{G^2F\mu_1}}}^{\infty}\Phi\left[\frac{\sqrt{G^2F\mu_1}\,z-(y_T-G\mu_1-\mu_g)}{\sigma}\right]P_{PDZ}(z|\mu_1)dz\\&=\int_{\frac{-G\mu_1}{\sqrt{G^2F\mu_1}}}^{\infty}\Phi\left[\frac{\sqrt{G^2F\mu_1}\,z-Y_T\sqrt{G^2F\mu_0+\sigma^2}+(G\mu_1-G\mu_0-\mu_g)}{\sigma}\right]P_{PDZ}(z|\mu_1)dz\end{aligned} \qquad (14)$$

where Y_T is the normalized threshold defined in (10).

SL6140

400MHz WIDEBAND AGC AMPLIFIER

(Supersedes edition in September 1988 Linear IC Handbook)

The SL6140 is an integrated broadband AGC amplfier, designed on an advanced 3-micron all implanted bipolar process. The amplifier provides over 15dB of linear gain into 50Ω at 400MHz.

Accurate gain control is also provided with over 70dB of dynamic range.

The SL6140 provides over 45dB of voltage gain with an R_L of 1kΩ.

FEATURES

- 400MHz Bandwidth ($R_L = 50\Omega$)
- High Voltage Gain 45dB ($R_L = 1k\Omega$)
- 70dB Gain Control Range
- High Output Level at Low Gain
- Accurate Gain Control
- Full Military Temperature Range (CM only)
- MC1590 Replacement with Improved Performance

APPLICATIONS

- RF/IF Amplifier
- High Gain Mixers
- Video Amplifiers

ORDERING INFORMATION

SL6140 NA MP
SL6140 A CM
SL6140 B CM
SL6140AC CM

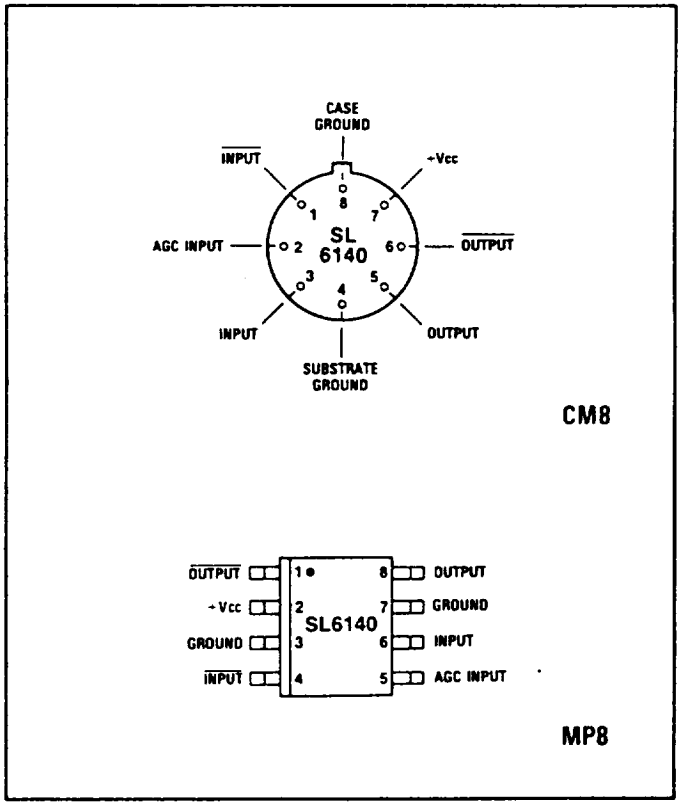

Fig.1 Pin connections (top view)

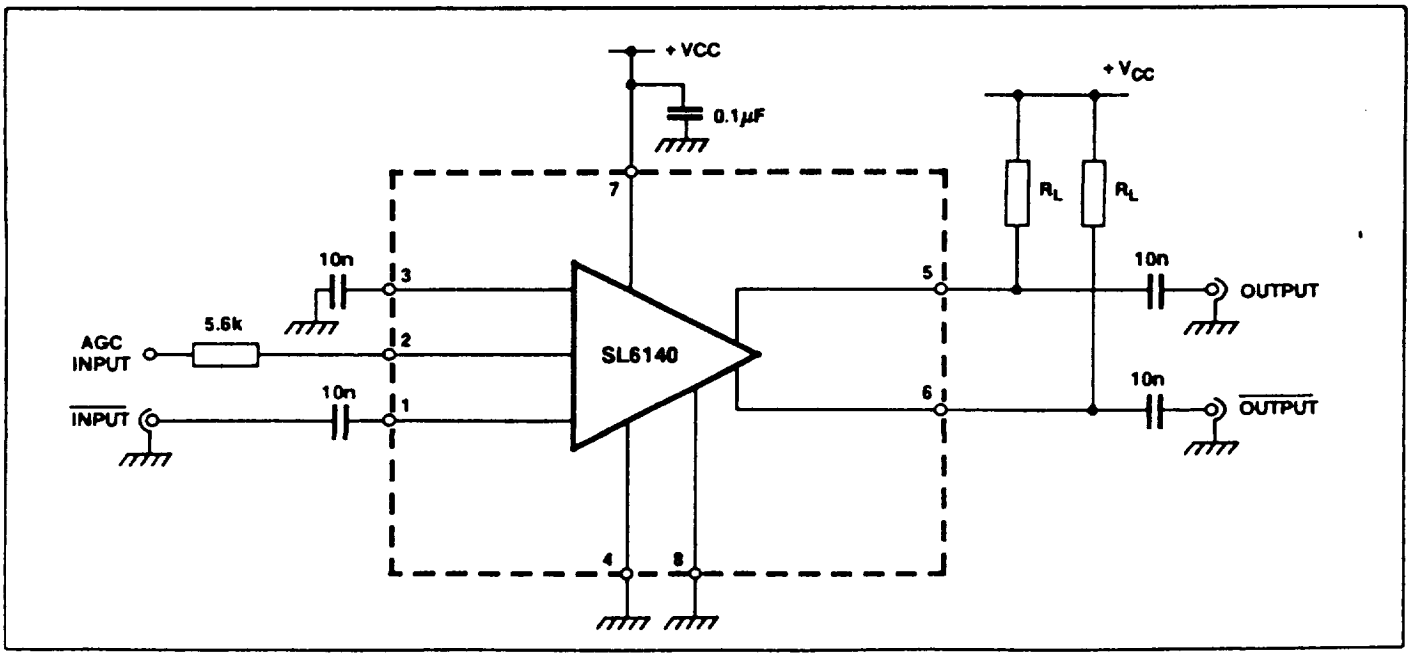

Fig.2 Typical wideband application (CM pinout)

ELECTRICAL CHARACTERISTICS

Test conditions (unless otherwise stated):
T_{amb} = 25°C, V_{CC} = + 12V

Characteristic	Pin	Value			Units	Conditions
		Min	Typ	Max		
Supply current	5,6,7	-	19	23	mA	
Output stage current	5,6 (sum)	5	7	9	mA	
Output current matching (magnitude of difference of output currents)	5,6	-	0.5	-	mA	
AGC range	2	60	75	-	dB	See Fig. 4 & Note 1
Voltage gain (single ended)	5,6	40	45	-	dB	R_L = 1kΩ See Fig.5 & Note 1
			55		dB	Tuned input and output
	5,6	-	15	-	dB	R_L = 50Ω
Bandwidth (-3dB)	5,6	-	25	-	MHz	R_L = 1kΩ See Fig. 5
			400		MHz	R_L = 50Ω
Maximum output level (single ended)						
0dB AGC	5,6	2.5	3.5	-	V p-p	Note 1
-30dB AGC	5,6	2.5	3.5	-	V p-p	R_L = 1kΩ, Note 1

NOTE 1. Guaranteed but not tested for MP package

DESCRIPTION

The SL6140 (Fig.3) is a high gain amplifier with an AGC control capable of reducing the gain of the amplifier by over 70dB. The gain is adjustable by applying a voltage to the AGC input via an external resistor (R_{AGC}), the value of which adjusts the curve of gain reduction versus control voltage (see Fig. 4) As the output stage of the amplifier is an open collector the maximum voltage gain is determined by R_L. With load resistance of 1kΩ the single ended voltage gain is 45dB and with a load resistance of 50Ω the voltage gain is 15dB ($20\log_{10} V_{OUT}/V_{IN}$). Another parameter that depends on the load resistance is the bandwidth: 25MHz for R_L = 1kΩ, as compared with 400MHz for R_L = 50Ω. R_L is chosen to give either the required bandwidth or voltage gain for the circuit.

Fig. 7 shows the input impedance of the device. Accurate impedance matching to both inputs and outputs of this device (by resonant circuit or other means) can raise the gain to 55dB but for most circumstances a 50Ω source impedance is adequate.

ABSOLUTE MAXIMUM RATINGS

Supply voltage, V_{CC}	+ 18V
Input voltage (differential)	+ 5V
AGC Supply	V_{CC}
Storage temperature	-55°C to + 150°C
Operating temperature	
SL6140 MP	0°C to 70°C
SL6140 B CM	-40°C to + 85°C
SL6140 A CM	-55°C to + 125°C
Chip operating temperature	
SL6140 MP	+ 175°C
SL6140 (CM variants)	+ 150°C

THERMAL RESISTANCE

Chip-to-ambient	
SL6140 MP	225°C/W
SL6140 (CM variants)	163°C/W
Chip-to-case	
SL6140 MP	65°C/W
SL6140 (CM variants)	57°C/W

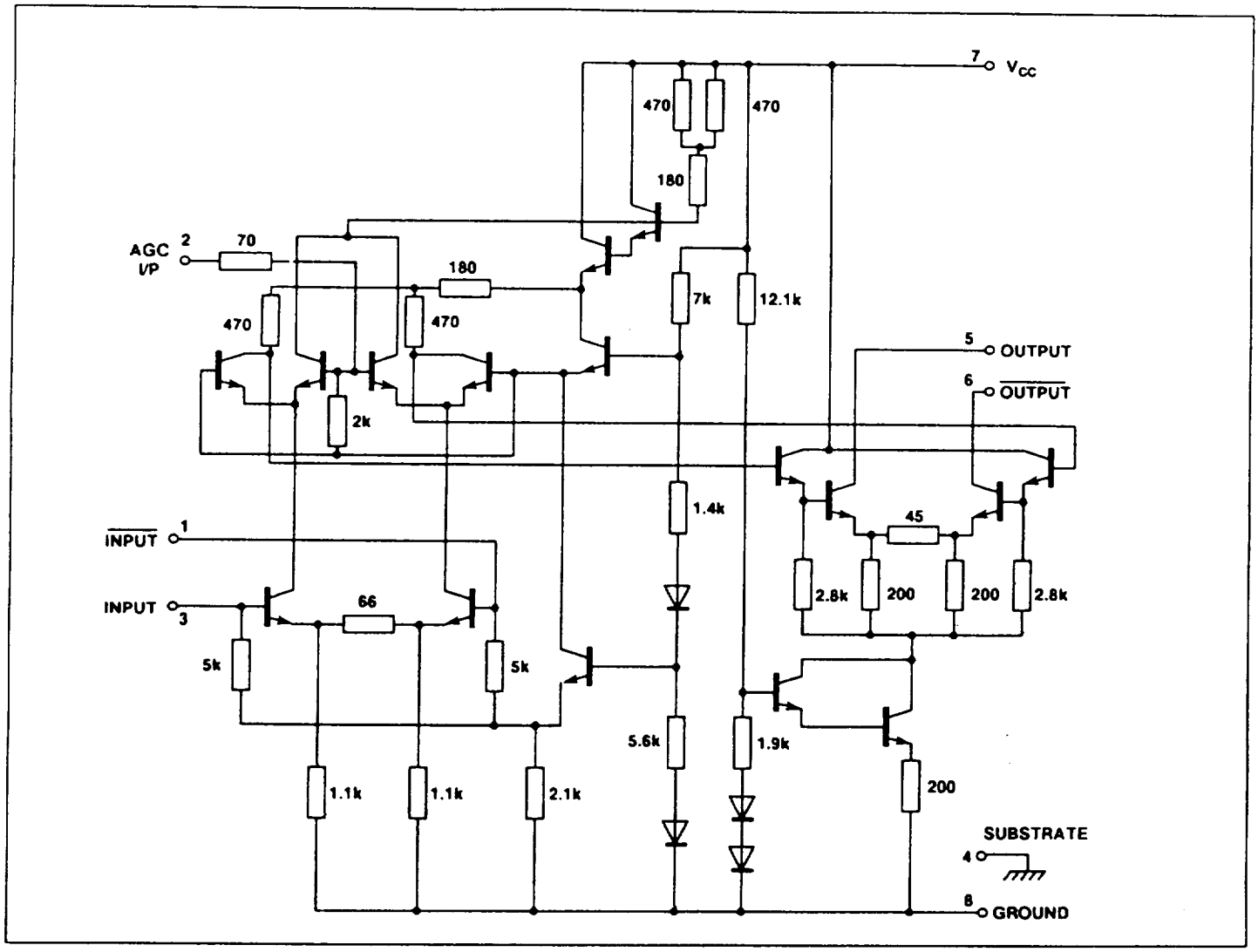

Fig. 3 - Full circuit diagram of SL6140 (CM pinout)

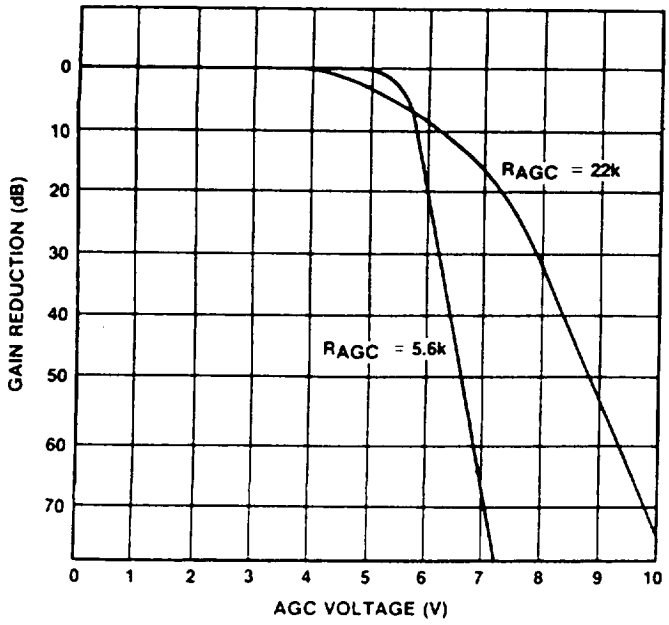

Fig 4 Gain reduction v. AGC voltage

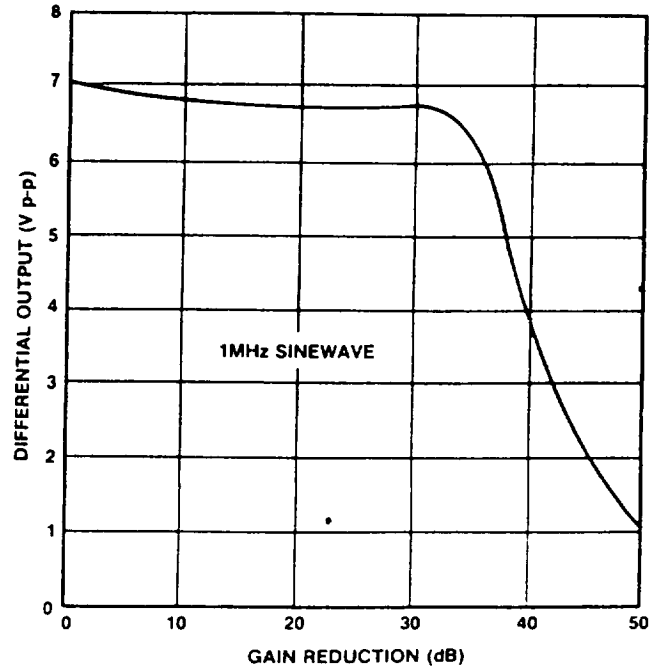

Fig 5 Voltage gain v. frequency

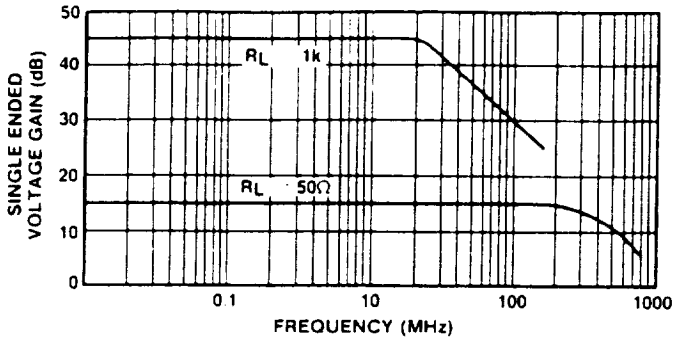

Fig 6 Maximum differential output v gain reduction

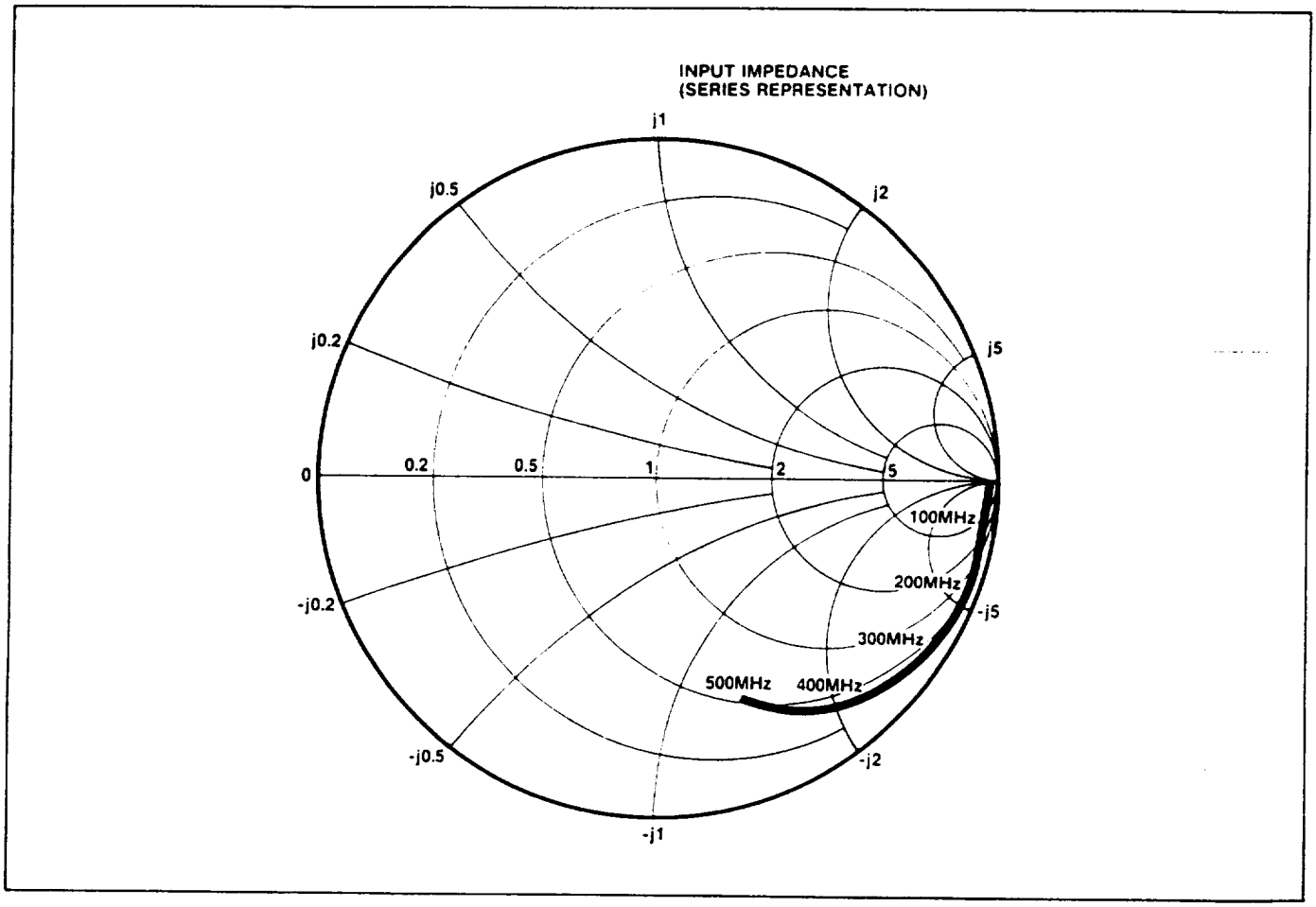

Fig 7 Input impedance of SL6140 (50Ω normalised)

GLAS Master Oscillator Frequency Determinization

Christopher T. Field

October 17, 1996

The GLAS instrument is a laser altimeter designed to measure the satellite altitude above the ground by measuring the time for a light pulse to travel to the ground and back. The range is to be measured to 7 cm from the 600 to 700 km orbit. There are many factors in the error budget; I allocate 0.7 cm to clock frequency error. Therefore, the frequency of the GLAS timing oscillator must be known to 7 mm/700 km or one part in 10^8. The GLAS mission is expected to last 5 years so the oscillator frequency must change slower than one part in 5×10^8 per year or there must be a way to account for the change in frequency. This performance is near the limits of state of the art crystal oscillator performance.

This report examines some of the factors involved in using on board GPS to provide time information which can be used to measure or control the master oscillator frequency. If sufficiently accurate frequency information can be determined, then the master oscillator may be of ordinary stability which decreases its cost and increases its reliability.

In addition to knowing the master oscillator frequency, the position of the laser spot on the ground must be known to 3 meters. This requires that the position of the exit aperture must be known to a fraction of a meter at the moment the laser fires. The satellite is moving at about 7 km/sec, or 7 m/msec. Assuming the orbit is known, knowledge of the time at which the laser fires to 0.1 msec enables precise knowledge of the exit aperture position. Consequently it would be helpful to synchronize (phase lock?) the master oscillator to GPS time.

Tracking four GPS satellites permits time and position to be determined, called 3D mode. If the receive's location is known, then only one satellite is required to determine time. This is known as 1D mode. Additional satellites

over determine the solution and permit a least squares solution with a smaller position and/or time error variance since most errors from each GPS satellite are independent. Each satellite dithers its signal to provide time and location uncertainty. The satellite dithers are independent of each other and has a power spectrum extending from about 1 Hz to 0.5 mHz (1/2 hour period). Including extra satellites in the solution reduces the time and position effects of the dither. From the ground, between 4 and 7 satellites are visible. From low earth orbit, Tom Clark says at least 12 GPS satellites should be visible. While the dithers are not known in real time, their errors can be further reduced by post processing on the ground.

Tom Clark has developed the Totally Accurate Clock (TAC) to replace or augment atomic clocks in remote sights. The TAC is a small GPS receiver (Motorola's ONCORE (PVT-6) OEM GPS receiver) which generates a pulse once each second. ONCORE is a six channel receiver which means it can track six satellites. Tom has done experiments comparing the difference between the GPS 1 PPS and the 1 PPS generated by various atomic standards. It is known that the ONCORE has an inherent jitter of ± 50 ns so Tom computes an average over 30 sec of the time difference between the PPS signals. In 3D mode, the 30 second average GPS 1 PPS has a peak jitter of ± 500 ns around perfect 1 PPS timing. When in 1D mode, the 30 second average difference drops to ± 100 ns peak with an RMS error less than 40 ns.

There are several ways to incorporate GPS time information for oscillator frequency measurement. The GPS 1 PPS may be used to measure either the master oscillator frequency or its period. Additionally the GPS signal may be used to steer the master oscillator to the desired frequency. Frequency measurement can be done by using the GPS 1 PPS to gate a running counter, one which is never reset, which counts cycles of the master oscillator. Each latched value is reported to the ground. The difference between consecutive readings is the number of oscillator cycles between the readings (in one second) from which the oscillator frequency can be determined. The average frequency over a given, sufficiently long period is easily determined. To measure the period, the master oscillator can be divided to yield 1 PPS. The period can be determined from measurement of the time interval between the master PPS and GPS PPS. Active frequency control, provides a frequency feedback to change the oscillator frequency as it deviates from the desired rate. Ideally information on changes to the control signal are provided to the ground along with the satellite status information.

The GLAS instrument requires several clock signals. There is an 800 MHz

signal to trigger the analog to digital converters, 50 MHz for the range gate, 25 MHz for the digital signal processor, 5 or 2.5 MHz for the cloud channel, and 40 Hz for the laser trigger. These signals will be derived synchronously from one master oscillator by a digital divider chain. The general plan is to use the GPS 1 PPS and the divider chain to measure either the oscillator frequency or period.

Before examining particular ways to measure frequency, here are some general definitions. Let the master oscillator have frequency f_o. The GPS 1 PPS has time jitter which makes the rising edge of the 1 PPS occur at times $t_0, t_1, \cdots$. Ideally, the times are given by $t_i = i\Delta T$ where $\Delta T = 1$ sec., but in fact are given by $t_i = i\Delta T + \delta_i$ where δ_i is the jitter of the i'th edge. It will be assumed that $\delta_i \ll \Delta T$, Gaussian distributed with zero mean and statistically independent.

For the frequency measurement approach, let the master oscillator drive a running counter, one which is never reset. At the leading edge of the GPS PPS, the counter value is latched to yield a value n. Let the set of observations $n_0, n_1, \cdots, n_M$ be made at times $t_0, t_1, \cdots, t_M$. Assume that the master oscillator frequency, f_o, is constant but unknown. Then

$$n_i = n_0 + (i\Delta T + \delta_i - \delta_0) f_o \tag{1}$$

where δ_i is zero mean Gaussian distributed with variance σ_δ^2. Then the difference between the counter values at observation i and j is given by

$$n_i - n_j = [(i-j) + \delta_i - \delta_j]\Delta T f_o \tag{2}$$

The estimated frequency during a single interval, (t_i, t_j) is given by

$$\tilde{f}_{o(i,j)} = \frac{n_i - n_j}{(i-j)\Delta T} \tag{3a}$$

$$= \left(1 + \frac{\delta_i - \delta_j}{(i-j)\Delta T}\right) f_o \tag{3b}$$

By inspection, the expected value of $\tilde{f}_{o(i,j)}$ is given by $E\left\{\tilde{f}_{o(i,j)}\right\} = f_o$ and (3b) provides an unbiased [1] estimate of the master oscillator frequency during the time interval. The variance of the estimated frequency is

$$\sigma_{\tilde{f}_o}^2 = E\left\{\tilde{f}_{o(i,j)}^{\,2}\right\} - E^2\left\{\tilde{f}_{o(i,j)}\right\} \tag{4a}$$

$$= \frac{2\sigma_\delta^2}{(i-j)^2\Delta T^2} f_o^2 \tag{4b}$$

which shows that the frequency estimate standard deviation drops as the the observation time interval increases.

Counter values will be recorded each second for M seconds which yields $M' = M+1$ counter readings which can be processed in several way. Adjacent counter values can be used to compute M one second frequency estimates which are averaged or $(M+1)/2$ frequency estimates can be computed from pairs and those values averaged. As shown below, for reasonable value of M the second approach yields a lower variance for the frequency estimate. Let the M' counter readings be made at times $\delta_0, 1+\delta_1, \cdots, M+\delta_M$. Between adjacent readings, a frequency estimate is made. The average estimate of frequency over the time t_0 to t_M is given by

$$\tilde{f}_o = \frac{1}{M}\sum_{i=1}^{M}\frac{n_i - n_{i-1}}{\Delta T} \tag{5a}$$

But because the counters are not reset after each reading all of the n values cancel except the first and last so

$$\tilde{f}_o = \frac{n_M - n_0}{M\Delta T} \tag{5b}$$

$$= \left(1 + \frac{\delta_M - \delta_0}{M\Delta T}\right) f_0 \tag{5c}$$

As before, because the δ's are zero mean this is an unbiased frequency estimate. The variance of the frequency estimate is computed as follows.

$$\sigma^2_{\tilde{f}_o} = E\left\{\left[\frac{1}{M}\sum_{i=1}^{M}\frac{n_i - n_{i-1}}{\Delta T}\right]^2\right\} - E^2\left\{\tilde{f}_o\right\} \tag{6a}$$

Again, all of the n's except the first and last cancel so

$$\sigma^2_{\tilde{f}_o} = \frac{2\sigma^2_\delta}{(M\Delta T)^2} f_o^2 \tag{6b}$$

Only the first and last count are needed to perform the average and the intermediate readings don't reduce the estimate variance.

An alternative approach permits contribution from all of the count readings and permits a smaller variance for the frequency estimate. Suppose that $M' = M+1$ is even. The readings can be grouped into $M'/2$ pairs spaced $\Delta i \Delta T$ apart. Then there are $M'/2$ estimates of frequency each given by

$(n_{i'+\Delta i}-n_{i'})/(\Delta i\Delta T)$ where the i's do not have to be time ordered. For example for $\Delta i = 1$, the $i' = 1, 2, 3, \cdots, M'/2$ correspond to $i = 0, 2, 4, \cdots, M-1$. The average estimated frequency is given by

$$\tilde{f}_o = \frac{1}{M'/2}\sum_{i'=1}^{M'/2}\frac{n_{(i'+\Delta i)}-n_{i'}}{\Delta i\Delta T} \tag{7a}$$

$$= \frac{1}{M'/2}\sum_{i'=1}^{M'/2}\left(1+\frac{\delta_{(i'+\Delta i)}-\delta_{i'}}{\Delta i\Delta T}\right)f_o \tag{7b}$$

Once again, (7b) is an unbiased estimate of the frequency. However, because each observation is included in the sum only once, the estimate variance, may be smaller than before. Taking into account that the δ_i's are zero mean and statistically independent, the variance is given by

$$\sigma^2_{\tilde{f}_o} = E\left\{\left[\frac{1}{M'/2}\sum_{i'=1}^{M'/2}\frac{n_{(i'+\Delta i)}-n_{i'}}{\Delta i\Delta T}\right]^2\right\} - E^2\left\{\tilde{f}_o\right\} \tag{8a}$$

$$= \frac{1}{M'/2}\frac{2\sigma^2_\delta}{(\Delta i\Delta T)^2}f_o^2 \tag{8b}$$

The interval Δi must be between 1 and $M'/2$. Clearly using the largest possible value of Δi produces the lowest variance given by

$$\sigma^2_{\tilde{f}_o} = \frac{8}{M'}\frac{2\sigma^2_\delta}{(M'\Delta T)^2}f_o^2 \tag{8c}$$

Therefore for $M' > 5$ using all of the readings to produce $M'/2$ frequency estimates provides a lower variance and hence a more efficient estimate of the oscillator frequency than using the first and last readings only.

An alternative approach measures the master oscillator period. Assume f_o/N is nearly 1 Hz. The terminal count from a divide by N counter will also be nearly 1 PPS. Call this signal the master PPS. See Figure 1. At time $t_i = i\Delta T + \delta_i$, let $\Delta t_i + \delta_{\Delta t_i}$ be the measured time between the master PPS and the GPS PPS where Δt_i is the true time interval and $\delta_{\Delta t_i}$ is the error in the interval measurement. The period of the master PPS is $P_o = N/f_o$ so, at time t_i the true time interval will be $\Delta t_i = (t_i - t_0) - k_{(i,0)}P_o/N$ and the measured time interval will be $\Delta t_i + \delta_{\Delta t_i} = (t_i - t_0) + \delta_{\Delta t_i} - k_{(i,0)}P_o/N$ where $k_{(j,0)}$ is the number of master oscillator cycles between t_i and t_0. Generally $k_{(i,0)} = i$ but it may be different because of cycle slips. An estimate of the

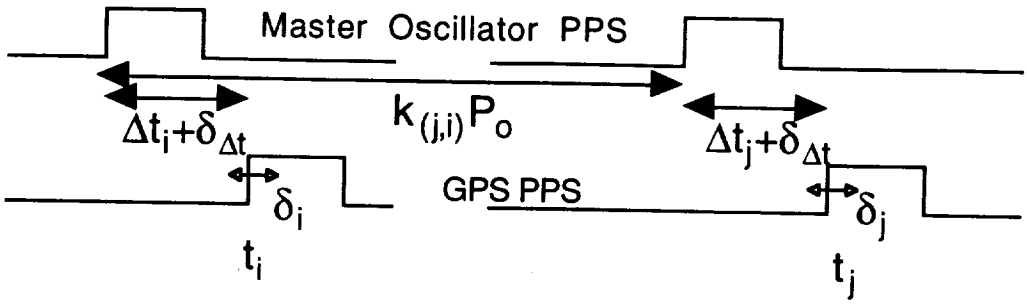

Figure 1: Picture showing the time relationships between 1 PPS from the GPS and the master oscillator divide by N counter.

average master oscillator period is given by

$$\tilde{P}_{o(j,i)} = \frac{(t_j - t_i) + (\Delta t_j - \Delta t_i)}{k_{(j,i)}} N \tag{9a}$$

$$= \frac{(i-j)\Delta T + (\delta_i - \delta_j) + (\Delta t_j - \Delta t_i) + (\delta_{\Delta t_j} - \delta_{\Delta t_i})}{k_{(j,i)}} N \tag{9b}$$

where $k_{(j,i)} = k_{(j,0)} - k_{(i,0)}$. Because the δ's are zero mean and assuming that $\delta_{\Delta t_i}$ are also zero mean, this is an unbiased estimate of the period. The variance of the period measurement is given by

$$\sigma^2_{P_o} = [2\sigma^2_\delta + 2\sigma^2_{\Delta t}] \frac{N^2}{k^2_{(j,i)}} \tag{10}$$

where $\sigma^2_{\Delta t}$ is the variance of $\delta_{\Delta t}$.

As before, multiple time interval readings may be averaged in several ways. The straight average of $\tilde{P}_{o(i,i-1)}$ for $i = 1, 2, 3, \cdots, M$ yields the average and variance of the single pair of observations at time t_0 and t_M as before and will not be investigated further. Using the alternative approach from before, the interval measurements may be paired with each value used only once. The average period is then be given by

$$\tilde{P}_o = \frac{1}{M'/2} \sum_{i'=1}^{M'/2} \tilde{P}_{o(i'+\Delta i,i)} \tag{11}$$

The variance of the estimate in (11) is calculated as before.

$$\sigma^2_{\tilde{P}_o} = E\left\{\tilde{f}_o^{\,2}\right\} - E^2\left\{\tilde{f}_o\right\} \tag{12a}$$

$$= \frac{1}{M'/2}\frac{2\sigma_\delta^2 + 2\sigma_{\Delta t}^2}{k^2_{(i'+\Delta i,i)}}N^2 \tag{12b}$$

If the frequency of the two oscillators are well matched and the timing jitter is not too large, $k_{(i'+\Delta i,i)}$ can be bounded by $1 \leq k_{(i'+\Delta i,i)} \leq M'/2$. Once again, the smallest variance is achieved by the largest value of $k \approx M'/2$. Therefore the variance of the period estimate is given by

$$\sigma^2_{\tilde{P}_o} \approx \frac{8}{M'}\frac{2\sigma_\delta^2 + 2\sigma_{\Delta t}^2}{M'^2}N^2 \tag{12c}$$

The time interval between the two 1 PPS readings does not have to be measured with high accuracy because the required precision is provided by having a large value of $i - j$ rather than high precision for Δt. The time interval is measured over a maximum of one second. Therefore, clock errors do not accumulate. If the timing clock is running fast by one part in 10^7, the maximum interval error will be 100 nsec, less than the likely GPS PPS jitter in 3D mode. This error is likely to be similar for the interval at each end of the sampling time and cancel out. But even if it does not cancel, increasing Δi will decrease the error in the master oscillator period measurement arbitrarily. Consequently ΔT_i may be measured with a "low accuracy" clock such as the master oscillator itself and a separate oscillator is not required.

The time interval is measured by starting a high frequency counter when the divide by N counter reaches zero and stopping (latching) it on the GPS PPS leading edge. But if the divide by N counter is a count up counter, it is zero when the master oscillator PPS is generated and its value when the GPS leading edge comes is the number of master oscillator cycles in the time interval. Therefore let n_i be the value of the divide by N counter when the GPS leading edge comes. Then $\Delta t_i = (n_i \pm 1)/f_0$ where the $\pm$ accounts for the single count uncertainty. Using a 10 MHz counter, ΔT can be measured to one part in 10^7 and master oscillator drift of a few parts in 10^8 will not be important. Consequently no additional oscillators or electronics are needed to measure the lag time. This system then performs just the same as the previous one which latches the value of running counters. This system has the additional advantage that it always reports the time difference between the master oscillator, hence the laser firing time, and GPS time which simplifies determinization of the laser spatial position when it fired.

Glenn Lightsey and I have spoken about four space qualified GPS receivers. The Jet Propulsion Lab (JPL) is developing the Turbo Rogu, Trimbol Navigation has the Vector, Space Systems Loral has the Tensor, and Trimbol and Honeywell are developing a new, unnamed, receiver.

The Turbo Rogu is a dual frequency receiver developed to probe the atmosphere by measuring the ionic delay as GPS satellites move above or below the horizon. The Turbo Rogu does not have attitude measuring capability and was not intended as the principle navigation receiver. The Turo Rogu has flown on a few small missions.

The Vector by Trimbol Navigation is a commercial development which uses commercial parts. It is a six channel receiver capable of reporting time, position, and attitude. It is a low cost unit, $30,000 and has flown 6 times. The typical orbits have been 800 km and lifetime was 6 to 18 months. Although the functions required for GLAS are there, the lifetime is not.

Space System Loral took the Trimbol Navigation design and engineered it for space flight. The Tensor (do you see a pattern here?) is a fully redundant 9 channel unit designed to provide time, position, and attitude for 5 years through 100 krad radiation. The Tensor costs about $500,000.

Trimbol in cooperation with Honeywell and GSFC Code 712 is developing another GPS receiver to cost about $100,000 and provide the functions of the Tensor but may not have quite the lifetime.

Many GPS receivers, including the ones above, provide a 1 PPS output which can be used by the circuits described in this paper to measure a crystal oscillator frequency. In orbit, the rising edge of the Tensor's 1 PPS signal is expected to be within 1μsec of the absolute time point. With post processing, it is possible to reduce the uncertainty of the edge location. With 1μsec timing uncertainty, the observation time must be 100 to 1000 seconds long to provide frequency or period knowledge to one part in 10^8.

I thank Bryan Blair, Tom Clark, and Glenn Lightsey all of Goddard Space Flight Center for providing extensive background information on GPS receivers and position determination.

More information on the TAC can be found on the Wide World Web at ftp://aleph.gsfc.nasa.gov/GPS/totally.accurate.clock/

References

[1] Walpole, Ronald E. and Myers, Raymond H. *Probability and Statistics for Engineers and Scientists* Macmillan Publishing Co, New York, (1978)